New Insight into Hexokinase-VDAC Interactions in a Fungal System

By

Jason Dubyna

A Thesis submitted to the Faculty of Graduate Studies of

The University of Manitoba

In partial fulfilment of the requirements of the degree of

MASTER OF SCIENCE

Department of Microbiology

University of Manitoba

Winnipeg

Abstract

Hexokinase and VDAC are two critical proteins throughout fungi. Despite the considerable number of studies on VDAC-hexokinase interactions in animal systems, little research has been attempted looking at their interaction in fungal systems. The existing work described in the literature suggests that yeast hexokinase and VDAC have no interaction, unlike in mammalian and plant systems. However, previous research used crude methods to test binding interactions and it has not been re-examined until recently, when Ferens *et al.* (Ferens et al., 2019) used detergent-solubilized *Neurospora crassa* VDAC and *Saccharomyces cerevisiae* (yeast) hexokinase to demonstrate that hexokinase isoform 1 (Hxk1) was capable of binding and hexokinase 2 (Hxk2) was not. The current work sought first to overexpress and purify the hexokinase isoforms from yeast to confirm that hexokinase 1 binds to VDAC and hexokinase 2 does not. This was achieved and binding affinities were determined using Microscale Thermophoresis. Hxk1 has a binding affinity for VDAC of 31.6 +/- 15.6 µM, whereas Hxk2 did not bind. The second goal was to determine the region of hexokinase 1 that is responsible for the isoform-specific binding. The two isozymes are very similar except for a few discrete regions. Variants were created by swapping short amino acid sequences from the Hxk1 binding isoform into the Hxk2 isoform. Hxk25-34, in which residues 25-34 were replaced with those from Hxk1, had a binding affinity close to that of Hxk1. Therefore, altering one small region of Hxk2 imparted binding affinity to VDAC. Our work opens potential avenues into investigating the functions of fungal VDAC-hexokinase interactions involved in gene regulation during glucose repression in yeast, a process in which hexokinases are involved.

Acknowledgments

I would like to thank the funding agency that allowed the work the work to be accomplished. The work was funded through the Natural Sciences and Engineering Research Council of Canada through NSERC grants that were awarded to my supervisor Deborah Court.

I would like to thank the Stetefeld, Prehna, and Mark labs in which I worked in their labs a fair amount at different points and their help and expertise which valuable many times.

The work would have never been possible without the help of my supervisor Deborah Court. She was extremely helpful with everything from start to finish from helping with my work, to answering questions, to asking questions, and anything else that I needed to finish my work. I would also like to thank my advisory committee, Dr. Ivan Oresnik, and Dr. Jörg Stetefeld for all their support and comments.

Table of Contents

List of Abbreviations

AEBSF	4-(2-aminoethyl)benzenesulfonyl fluoride hydrochloride
ATP	Adenine tri-phosphate
CCR	Carbon Catabolite Repression
CHS	Cholesteryl-hemisuccinate
DM	n-decyl-β-d-maltopyranoside
G6PI	Phosphoglucoisomerase
G6PD	Glucose-6-phosphate dehydrogenase
Gal	Galactose
Gal1	Galactose inducible promoter
Glc7-Reg	Glycogen phosphatase
Glk1	Glucokinase
Glu	Glucose
His_6	Six subsequent histidine tag.
Hk	Mammalian hexokinase
IMP	Integral membrane protein
K_d	Dissociation constant
Mig1	Multicopy inhibitor of GAL gene expression I
Mig2	Multicopy inhibitor of GAL gene expression II
MOM	Mitochondrial outer membrane
MOPS	3-(N-morpholino)propanesulfonic acid, 4-(N-morpholino) propanesulfonic acid
MST	Microscale thermophoresis
ncVDAC	*Neurospora crassa* Voltage Dependent Anion Channel
PDB	Protein data bank
pESC	Plasmid for protein expression in yeast

pET21b	Plasmid for protein expression in *E. coli*
SC	Synthetic Complete media everything needed for Ry13 yeast growth
SD	Synthetic Defined missing a component needed for RY13 growth
SEC	Size exclusion chromatography
Snf1	Sucrose non-fermenting I
Suc2	Sucrose II
VDAC	Voltage Dependent Anion Channel
$VDAC^R$	Recombinant refolded VDAC
yHxkI	*Saccharomyces cerevisiae* hexokinase I
yHxk2	*Saccharomyces cerevisiae* hexokinase II
Ura	Uracil

List of Figures

Chapter 1: Literature Review

1 Introduction

Voltage dependent anion channel (VDAC) and hexokinase are two extremely important proteins in eukaryotes (Mazure, 2017). The interaction between these proteins has been shown to be vital for cellular regulation of metabolism and apoptosis in mammalian cells (Mazure, 2017; Pastorino & Hoek, 2008; Shoshan-Barmatz et al., 2020). There is a lack of consensus as to how or if these two proteins interact in fungi (Aflalo & Azoulay, 1998; Forte et al., 1987; Pastorino & Hoek, 2008). In this review hexokinase and VDAC will be discussed generally, and more specifically what is known about yeast hexokinase regulatory processes will be described. Also, this review will examine how mammalian hexokinase binds to VDAC and what is different about mammalian and yeast hexokinase. Then lastly, this review will examine whether yeast hexokinase and VDAC also interact.

1.1 An overview of Hexokinase

Hexokinases are regulatory and enzymatic proteins that are highly conserved across eukaryotic species (Kuser et al., 2008). A hexokinase (EC 2.7.1.1) catalyses the phosphorylation of a hexose sugar, such as glucose, to form a hexose-6-phosphate (reaction 1.1.1, (Magri et al., 2018; Pastorino et al., 2002)). This process requires ATP as the source of the phosphate group and magnesium as an activator for catalytic activity (Magri et al., 2018; Pastorino et al., 2002; Schmidt & Colowick, 1973).

$$D-glucose + ATP \xrightarrow{HXK} glucose-6-P + ADP \quad (1.1.1)$$

Saccharomyces cerevisiae (yeast) has three different enzymes capable of glucose phosphorylation (Randez-Gil et al., 1998). They are hexokinase I (Hxk1), hexokinase II (Hxk2), and glucokinase (Glk1) (Randez-Gil et al., 1998). The isoforms of Hxk are extremely similar in both structure and function (Kraakman et al., 1999). In addition to the catalytic functions of Hxk isoforms I and II, they have an important role in glucose repression (Pelaez et al., 2010; Vega et al., 2016). We framed our research on Hxk1 and Hxk2 because Glk1 does not share their regulatory processes (Vega et al., 2016).

Yeast hexokinases are involved in sugar metabolism by catalysing the first step in glycolysis and the expression of the different isoforms is dependent on the availability of glucose (Kayikci & Nielsen, 2015; Vega et al., 2016). *HXK1* expression is increased in the absence of glucose in the cell. In contrast, the expression of *HXK*2 is amplified in the presence of glucose. In high glucose conditions Hxk2 is involved in the repression of *HXK1* transcription (Kayikci & Nielsen, 2015; Vega et al., 2016) (see section 1.3 for details). This is because Hxk2 is the preferred isozyme when glucose or mannose is the substrate (Schmidt et al., 2020). Not only is yHxk2 more efficient for glucose than for fructose metabolism it is also required for glucose repression by binding Mig1 in the nucleus (Fernandez-Garcia et al., 2012; Kuser et al., 2008; Schmidt et al., 2020; Vega et al., 2016). On the other hand, in a *HXK2* null mutant Hxk1 can partially recover glucose repression during overexpression (Fernandez-Garcia et al., 2012; Schmidt et al., 2020; Vega et al., 2016). Essentially, when large quantity of Hxk1 is produced the Mig1 repressor complex would still form and prevent fructose catabolism genes from being

produced. However, when fructose is the sole carbon source both Hxk1 and Hxk2 are both able to cause fructose repression (Schmidt et al., 2020). This seems reasonable because Hxk1 has a specific activity that is around 2.6 times higher for fructose than for glucose and is more likely to be involved in fructose processes (Kuser et al., 2008). Based upon this yeast hexokinase 1 and 2 clearly substantive differences in catalysis and interaction leading to a possibility that one isoform and not the other could interact with VDAC.

1.2 Yeast Hexokinase Structure

Yeast hexokinases are ~55-kDa proteins (Aflalo & Azoulay, 1998) that exist in a monomer-dimer equilibrium (Easterby & Rosemeyer, 1972; Randez-Gil et al., 1998). The monomer of Hxk2 has been shown to have a higher binding affinity for glucose than the dimer does (Lazarus. N. et al., 1966; Randez-Gil et al., 1998). When glucose is absent, Hxk2 is phosphorylated on Ser^{15} at the N-terminus and this shifts the equilibrium to the monomeric form that has higher sugar-binding affinity (Fernandez-Garcia et al., 2012; Kraakman et al., 1999; Lazarus. N. et al., 1966). In the presence of glucose, Hxk2 becomes dephosphorylated (Fernandez-Garcia et al., 2012; Kraakman et al., 1999). Thus, in low levels of glucose, hexokinase equilibrium shifts to the form that is more efficient at binding sugars, which helps the cell utilize very limited amounts of glucose (Lazarus. N. et al., 1966; Randez-Gil et al., 1998). When the 15-residue N-terminal region of Hxk2 is deleted, dimers cannot be formed but the enzymatic function declines only by a small margin (Ma et al., 1989). Together these observations reveal the separate regulatory and catalytic functions of the enzyme.

Yeast hexokinase isoforms I and II share about 77% amino acid sequence identity with many large, conserved regions (Fig. 1.1, (Kuser et al., 2000). Many of these regions are extremely important to enzymatic function and are conserved not only across yeast but also in all domains of life (Kuser et al., 2008). Hxk1 has 485 residues and Hxk2 has 486 residues and both isoforms have the same 24-residue N-terminal sequence (Kuser et al., 2008). The isozymes act as phosphoproteins whereby the phosphorylation state at Ser^{15} impacts dimerization, catalytic activity, and binding interactions (Fernandez-Garcia et al., 2012; Kuser et al., 2008). Both isoenzymes are "palm" shaped, with the same α-helical and β-strand regions throughout (Kuser et al., 2008), Fig. 1.2). In contrast, mammalian cells have four hexokinase isoforms (Fig. 1.3) and three of these enzymes (Hk-I, Hk-II and Hk-III) have two large domains each the size of yeast hexokinase (Kuser et al., 2008). Both of these C- and N-terminal domains share sequence similarity with the yeast hexokinases, but not all are catalytic (Kuser et al., 2008). All secondary structure components in both yeast isoforms are shared by human hexokinases, except for the three extra 3_{10} regions in yeast (Kuser et al., 2000). These three regions are between amino acids 245-251, 269-273, and 445-449 (Fig. 1.2). These three regions are peripheral to the protein and not within the catalytic cleft. Therefore, it is possible these regions could have an impact on yeast specific regulation.

Figure 1. 1. Sequence alignment for *Saccharomyces cerevisiae* hexokinase.

Sequence alignment for *Saccharomyces cerevisiae* hexokinase I and II (SwissProt accession numbers P04806 and P04807, respectively). The middle row indicates the amino acid code if it is the same residue, is blank if it is different, and has a + if the residue is similar.

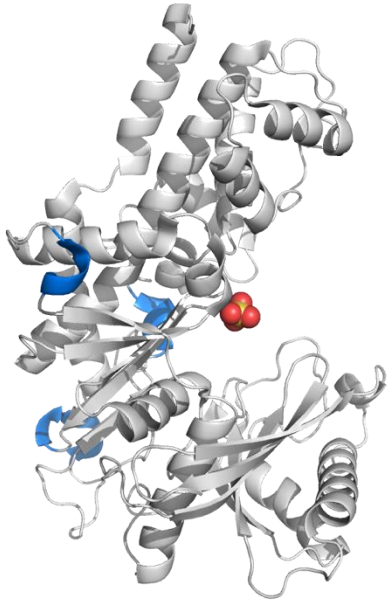

Figure 1. 2. *Saccharomyces cerevisiae* hexokinase II model.

Saccharomyces cerevisiae hexokinase II model created in PyMOL (PDB 1IG8, (Kuser et al., 2000)). The blue regions are amino acids 245-251, 269-273, and 445-449. These regions are 3_{10}-helices which are unique secondary structures not present in hexokinase from other species.

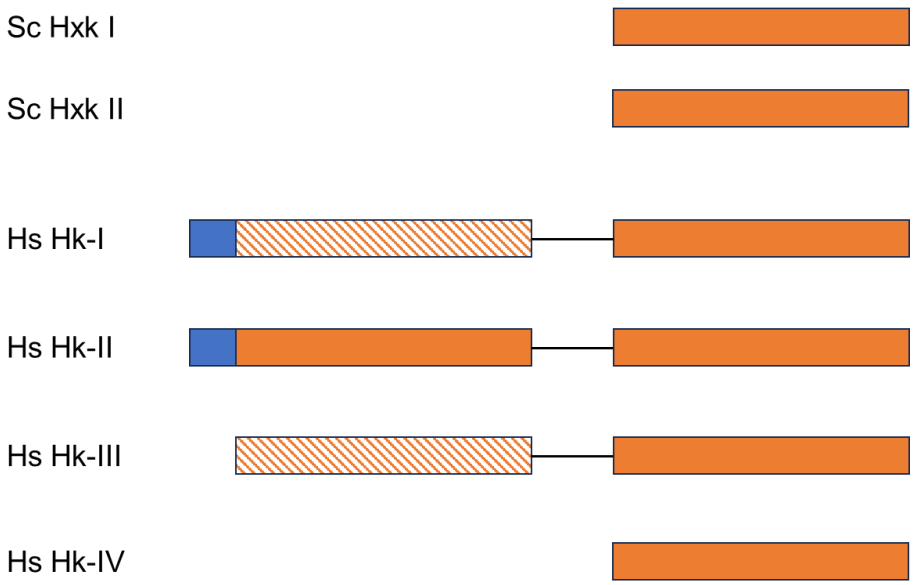

Figure 1. 3. Arrangement of domains in various hexokinase isoforms.

Arrangement of domains in various hexokinase isoforms. Hk-I, II and III from *Homo sapiens* have two kinase domains; solid bars indicate catalytically active domains and striped bars are enzymatically inactive, regulatory domains. The blue region is the hydrophobic (H) anchor required for mammalian hexokinase I and II to bind to VDAC1. Sc, *Saccharomyces cerevisiae;* Hs, *Homo sapiens.* Based on Roberts and Miyamoto (Roberts & Miyamoto, 2015).

Both yeast hexokinases consist of two distinct domains (Kuser et al., 2008). Between the two domains is a deep cleft that forms the active site where glucose binds and the most conserved sequences are located here (Fig. 1.4, (Kuser et al., 2008; Kuser et al., 2000). The catalytic cleft can be seen (Fig. 1.4) as the region around the phosphate group. There are residues that rotate, creating the open and closed conformations of the protein (Kuser et al., 2008). These residues are 74-103, 107-210, 212-213, and 459-477 in Hxk1 (Kuser et al., 2008).

Residues Asp^{211}, Gly^{215}, and Gly^{458} act as a mechanical hinge that allow a rotation angle of up to 17° (Kuser et al., 2008). When glucose is bound and Hxk1 in the closed formation Glu^{302}, Glu^{269}, and Lys^{176} hydrogen bond the glucose molecule (Kuser et al., 2008). The catalytic residue is Asp^{211}, and phosphate transfer is predicted to be facilitated by Ser^{158} (Kuser et al., 2008; Kuser et al., 2000).

1.3. Hexokinases and glucose repression in yeast

Saccharomyces cerevisiae is capable of massive metabolic flexibility because it can utilize many carbon sources through fermentation and non-fermentation pathways (Laurian et al., 2019). Yeast proteomics have shown that within 20 minutes of glucose addition, products of 20% of the 6200 genes in *S. cerevisiae* are altered three-fold and 40% are altered two-fold (Santangelo, 2006). This indicates a rapid and widespread regulatory system involved in carbon source utilization. In general, transcription of genes involved in alternative carbon source metabolism are shut off in the presence of glucose (Santangelo, 2006).

The most well-established role for yeast hexokinases in regulation is within glucose repression (Santangelo, 2006). Glucose repression is a process by which the presence of glucose in a cell alters its gene expression such that other carbon sources are not utilized (Kayikci & Nielsen, 2015; Santangelo, 2006)**.** *Saccharomyces cerevisiae* is capable of vastly altering the production of its gene products depending on the environmental conditions (Kayikci & Nielsen, 2015). Yeast prefers glucose over other carbon sources for ATP generation (Laurian et al., 2019). Therefore, yeast in the presence of glucose uses regulatory systems that prevent

utilization of other carbon sources as a means to be metabolically efficient (Kayikci & Nielsen, 2015). Hexokinase has been recognized as key in this regulatory process (Fernandez-Garcia et al., 2012; Kayikci & Nielsen, 2015; Randez-Gil et al., 1998; Vega et al., 2016). In a very general picture, *HXK*2 expression is increased in the presence of glucose and *HXK1* expression is decreased, and their relative concentrations have a regulatory impact (Kayikci & Nielsen, 2015). Hxk2 binds to the repressor Mig1 via the Lys^{6} to Met^{15} region and the resulting complex is translocated into the nucleus (Fernandez-Garcia et al., 2012; Pelaez et al., 2010). Once inside the nucleus Hxk2 forms part of a larger complex with Mig1 and Mig2 (Kayikci & Nielsen, 2015; Vega et al., 2016). Mig1 and Mig2 are Zinc-finger transcription repressors that bind the *SUC*2 promoter region and prevent transcription of this gene (Kayikci & Nielsen, 2015; Vega et al., 2016). *SUC*2 encodes for the sucrose transporter but the *SUC*2 region includes around 350 other genes (Vega et al., 2016) Hxk2 has been shown to be critical to this function and *HXK*2 deletion mutations have a massively reduced ability to inhibit alternative carbon source gene transcription (Vega et al., 2016). In high glucose conditions, Glc7-Reg, a phosphatase, dephosphorylates Mig1 and Hxk2, leading to the active complex that inhibits transcription of genes whose products are involved in utilization of alternative carbon sources (Kayikci & Nielsen, 2015; Vega et al., 2016). In low glucose conditions, Snf1 phosphorylates Mig1, leading to disassociation of yHxk2 and translocation out of the nucleus (Fernandez-Garcia et al., 2012; Kayikci & Nielsen, 2015; Vega et al., 2016). Using fluorescent microscopy to determine Hxk location *in vivo*, only Hxk2 has been shown to be in the nucleus (Fernandez-Garcia et al., 2012). However, Hxk2 deletion mutants are still capable of partial inhibition of the *SUC*2 gene, suggesting that Hxk1 is also capable of inhibiting alternative carbon source gene transcription

to a much smaller extent (Vega et al., 2016). Hxk1 is identical in the first 24 amino acids to Hxk2, including the region that binds to Mig1 (Vega et al., 2016), indicating that other differences between the proteins are involved in Mig1 binding or translocation to the nucleus. These observations highlight how yeast hexokinases are not only capable of regulation, but regulation is in fact a critical part of the protein's function (Vega et al., 2016).

Mutational studies have revealed that there are separate regions of Hxk2 responsible for the regulatory and catalytic functions (Kraakman et al., 1999; Pelaez et al., 2010). Peláez *et al.* (2010) created a Hxk2 variant S304F that also had the C-terminal eight amino acids deleted and this prevented the glycolytic function but not the regulatory function (Pelaez et al., 2010). Another variant had a deletion from Lys^{6} to Met^{15} and strains expressing this variant were still capable of glycolysis but were no longer capable of forming the Mig1 repressor complex at *SUC2* promoters (Pelaez et al., 2010). Therefore, the regions away from the catalytic cleft in Hxk2 likely have important regulatory functions (Kuser et al., 2008).

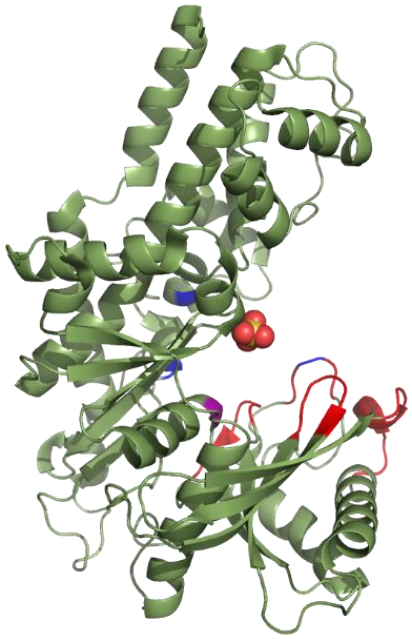

Figure 1. 4. *Saccharomyces cerevisiae* Hexokinase II model with highlighted catalytic sites. *Saccharomyces cerevisiae* Hexokinase II important interactional sites for glucose phosphorylation (PDB 1IG8, (Kuser et al., 2000). Residue Asp211 in purple is the catalytic residue. Residues Lys176, Glu269, and Glu302 in blue are the sugar binding residues. The residues in red are flexible domains capable of closing the left after glucose binding. Model created using PyMOL.

1.4 VDAC Overview

VDAC (Voltage Dependent Anion Channel) is an integral membrane protein (IMP) in the mitochondrial outer membrane (Summers & Court, 2010). IMPs are involved in many vital cellular processes, as well as being linked to human disease (Uhlen et al., 2015). They are difficult to study and less well-characterized than water soluble proteins, as evidenced by the

low number of protein data bank deposits for IMPs (Berman et al., 2000). IMPs have transmembrane domains that are formed by α-helices, or they exist as β-barrels (Muller et al., 2008). VDAC is composed of 19 transmembrane β-strands and an N-terminal α-helix (Fig. 1.5; (Bayrhuber et al., 2008; Hiller et al., 2008; Mazure, 2017; Ujwal et al., 2008).

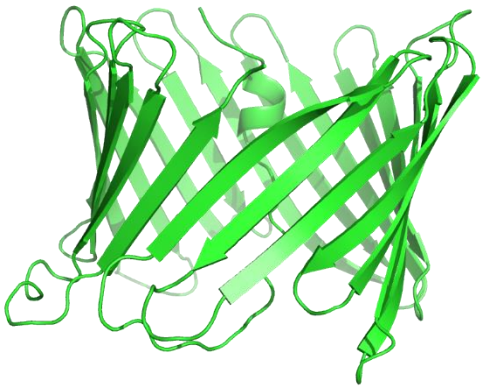

Figure 1. 5. *Neurospora crassa* model.

Neurospora crassa voltage-dependent anion channel predicted structure using Phyre2 (Kelley et al., 2015) modeling using the structure of human VDAC-1 in LDAO micelles (2K4T PDB). The N-terminal α-helix resides inside the barrel in this model.

VDAC have been found in all species of eukaryotes including yeast and are very abundant, comprising about 10% of the proteins in the outer membrane (Mazure, 2017). VDAC is a porin protein that allows the influx and efflux of ions and small metabolites from the mitochondria (Arzoine et al., 2009). Metabolite movement through VDAC is a highly regulated process across the eukaryotic domain of life and therefore VDAC is important for the survival and growth of the cell (Kuser et al., 2000). Due to VDAC's role in the flux of mitochondrial

metabolites, it is an important site for binding by other proteins such as hexokinase and creatine kinase in animals (Pastorino et al., 2002)**.**

In mammals, VDAC1 interacts with anti-apoptotic and pro-apoptotic proteins that regulate a cascade that causes cell death (Mazure, 2017; Pastorino & Hoek, 2008; Shoshan-Barmatz et al., 2020). Hexokinases 1 and 2 are capable of binding VDAC1 in mammals and leading to anti-apoptotic effects (Mazure, 2017; Pastorino & Hoek, 2008; Shoshan-Barmatz et al., 2020)(Hoek 2008, Mazure 2017). These effects can determine the fate of cancer cells (Mazure, 2017; Shoshan-Barmatz et al., 2020). In total, as a result of the pore-forming ability and the interactions with other proteins, VDAC is critical in many cellular processes such as apoptosis, metabolism, calcium homeostasis, and this wide-ranging control could lead to its connection to many diseases (Mazure, 2017; Shoshan-Barmatz et al., 2020). VDAC levels have been shown to be altered and potentially implicated in Alzheimer's, cancer, lupus, inflammatory bowel disease, and cardiac diseases (Mazure, 2017; Shoshan-Barmatz et al., 2020).

1.5 VDAC-Hxk binding

The interaction between hexokinase and VDAC has been well studied in mammalian cells (Shoshan-Barmatz et al., 2020). Hexokinase requires ATP in order to catalyze the reaction to glucose-6-phosphate (Magri et al., 2018) and ATP produced by oxidative phosphorylation exits the mitochondria via VDAC (Kovac et al., 1986), a process which can be tightly regulated by VDAC (Mazure, 2017) and proteins that bind to it (Pastorino & Hoek, 2008). Potentially the

requirement for ATP has led to hexokinase isoforms being associated with VDAC for preferential access to the release of ATP from the mitochondria (Haloi et al., 2021; Pastorino et al., 2002). Previous research on VDAC has focused on mammalian cancer cell lines and there have been few experiments focusing on fungal hexokinase isoforms and VDAC.

There are two main hypotheses for the mechanism of hexokinase-VDAC binding in mammalian systems, where HK-I and HK-II interact with one of the three isoforms of VDAC, namely VDAC1. The first of which is that the N-terminal domain of hexokinase 1 reaches into the barrel of VDAC and binds to the walls of the pore (Rosano, 2011). However, there are a few potential problems with this model, the first of which is that directly binding within the pore would likely block the channel (Haloi et al., 2021). The other problem is that there is an inherent mismatch between the hydrophobic H-anchor region of hexokinase and the highly charged interior VDAC1 surface (Haloi et al., 2021). In a VDAC1 null mutant, HK-II can still bind the mitochondria. If the H-anchor is truncated or removed from hexokinase it can no longer bind VDAC or VDAC-less mitochondria (Haloi et al., 2021). Therefore, the H-anchor of the hexokinase is required for binding and, residue S215 is also required for binding to VDAC1 (Haloi et al., 2021).

These results suggest a second model in which there more generalized binding both to the outer lip of VDAC but also in smaller part the adjacent membrane of mitochondria (Haloi et al., 2021). Using Brownian dynamics simulations, it was determined that HK-II anchored on a membrane mimetic could bind VDAC1 on the cytosolic surface (Haloi et al., 2021). Additionally, tests of bound HK-II to VDAC1 embedded in artificial membranes revealed a partial reduction in

conductance, suggesting that HK-II partially blocks the pore, or induces a change in its conformation (Haloi et al., 2021). Binding of the HK-II N-terminus within the pore would reduce the effective radius of the pore from 13 to 2.1 Å (Haloi et al., 2021). Under these conditions it would essentially be a complete blockage of metabolite flow, which was not seen (Haloi et al., 2021). Binding to the cytosolic lip of VDAC1 however, would lead to a smaller predicted decrease in pore size, from 13 to 7.3 Å (Haloi et al., 2021), which is more compatible with the electrophysiology data. Therefore, the model in which hexokinase binds to the outer rim of VDAC seems more likely (Haloi et al., 2021). Despite the importance of H-anchor of Hk-II in binding to VDAC, the removal of this segment does not completely prevent mitochondrial localization and binding (Rosano, 2011), supporting this model and suggesting that other regions of the protein are involved in interactions with VDAC1 that stabilize binding. Yeast hexokinases do not have the H-anchor portion that is present in mammals (Fig. 1.3), but given the previous observation, and the fact that yeast and mammalian hexokinases share homologous regions and the corresponding VDAC share positively charged surface loops (Bay et al., 2012), yeast hexokinase localization to the mitochondria or binding to VDAC may be possible despite not having the H-anchor. Finally, mammalian mitochondria lacking VDAC1 bind to mammalian hexokinase (Haloi et al., 2021), suggesting that hexokinase have some level of non-specific interaction the MOM and yeast hexokinase may bind yeast VDAC.

While an interaction between Hk-II and VDAC1 has been established in mammalian systems, a clear interaction in a fungal system has not been demonstrated (Pastorino & Hoek, 2008). Several experiments were done to attempt to determine if yeast hexokinase interacts with yeast mitochondria. Organelles were burst to determine if there is hexokinase association

with organelles or if it is purely cytosolic (Kovac et al., 1986). They tested during glucose repression and derepression and found that hexokinase locational values were the same as cytosolic proteins and unlike mitochondrial proteins (Kovac et al., 1986). Another experiment with purified yeast VDAC and hexokinase found no binding; however, the authors did not include the data or explain how this was done (Kovac et al., 1986). Another team determined that hexokinase could bind purified VDAC that was reconstituted into liposomes (Forte et al., 1987). They centrifuged the liposomes and found no hexokinase bound when VDAC was not embedded within the liposomes and did find it when VDAC was constituted into the liposomes (Forte et al., 1987). Aflalo et al. also examined purified hexokinase and mitochondria to determine affinity (Aflalo & Azoulay, 1998). They mixed the purified samples for one hour and centrifuged to determine bound and free hexokinase (Aflalo & Azoulay, 1998). They determined that yeast hexokinase either did not bind yeast mitochondria or VDAC or did at an extremely low level (Aflalo & Azoulay, 1998). All of these experiments suggest that it is not clear if yeast hexokinase and VDAC interact, and if it does, it is likely not a very strong interaction.

Some experiments have shown that mammalian hexokinase is capable of binding to yeast VDAC (Aflalo & Azoulay, 1998), but this heterologous system may not be representative of homologous interactions in fungi. The general conclusion from these assays is that yeast hexokinase either does not bind yeast VDAC or it binds with a much higher affinity than that of the mammalian versions (Lemeshko, 2017).

Therefore, research in a fungal model system could be extremely helpful in and of itself and to understand these proteins and their interactions in eukaryotes. Previous work in our lab

has shown that *S. cerevisiae* hexokinase I (HxkI) binds *Neurospora crassa* VDAC (ncVDAC) that is solubilized in micelles of the detergent decylmaltoside and cholesteryl-hemisuccinate (CHS); however, the other isoform, hexokinase II, (Hxk2) is not capable of binding (Ferens et al., 2019). These studies used a commercially available mixture of Hxk1 and Hxk2 and the isoforms were purified by anion exchange chromatography. A binding constant for ncVDAC and Hxk1 of 27 ± 6 µM was determined using microscale thermophoresis (MST) (Ferens et al., 2019). This system utilizes only purified proteins, which may enhance detection of weak interactions. We are not using a homologous system, however; ncVDAC and scVDAC1 are 42% identical at the amino acid sequence level, have segments with identical sequences, and shared charged patches on the outer surfaces of the pore (Bay et al., 2012). Likewise, *S. cerevisiae* hexokinase 2 has 26-55% sequence identity to the four enzymes with hexokinase activity in *Neurospora crassa*. Areas of proteins that are critical to proper cellular function tend to be conserved and a potential Hxk-VDAC interaction may be important to cell growth. Antibodies against *Saccharomyces cerevisiae* VDAC were also able to bind a number of other VDACs including *N. crassa* VDAC suggesting a functional and antigenic similarity (Forte et al., 1987). Mammalian and yeast VDACs have extremely low sequence homology in comparison and despite this rat hexokinase still has relatively high levels of binding to yeast VDAC (Aflalo & Azoulay, 1998). Therefore, *N. crassa* and *S. cerevisiae* proteins, which share much higher sequence identity would be even more likely to share similar binding affinities. Due to this, our heterologous system may be representative of a homologous system within *S. cerevisiae*.

To further investigate this isoform-specific binding, we wanted to determine which region within Hxk1 is required for binding. Yeast hexokinase I and hexokinase II each have a

single catalytic domain (Fig. 1.3.) and have primary sequences that are about 77% identical (Kuser et al., 2000). Large regions of the isozymes are almost entirely conserved (Fig. 1.1, (Kuser et al., 2000)). The remaining clusters of non-conserved residues are strong candidates for contributing to the specific binding.

1.6 Hexokinase Variants

In an attempt to identify the isoform-specific region(s) that are responsible for Hxk1 specific binding, Hxk2 variants were made by replacing amino acids 25-34, 25-48, 319-328, and 443-452 with the corresponding Hxk1 sequence to attempt to impart binding affinity. Previous work indicated that Hxk1 is able to bind to ncVDAC and Hxk2 is not capable of binding to ncVDAC (Ferens et al., 2019). Therefore, to determine what region(s) may be involved in the difference in binding between the isoforms, regions from Hxk1 were swapped into Hxk2 to attempt to impart binding affinity. The isoforms are 77% identical at the amino acid sequence level and the majority of the unique amino acids fall within a few compact regions. These regions were chosen as possible candidates for the specifying binding affinity, and it is important to consider their placement in the 3-dimensional structure of the enzyme.

Yeast hexokinase has two large domains both contributing towards catalytic and regulation functions of the protein (Kuser 2008). The catalytic region of the enzyme primarily exists within and around the catalytic cleft that can be viewed surrounding the phosphate molecule in Fig. 1.4 (Kuser et al., 2008; Kuser et al., 2000). The other regulatory regions exist in the outer surfaces of the enzyme (Kuser et al., 2008; Kuser et al., 2000). There are four

significant regions between Hxk1 and Hxk2 are non-conserved and they are labeled in Fig. 1.6. These regions all exist far from the catalytic cleft which is much more conserved and exist within the regulatory region. Therefore, since these three regions are exterior to the protein allowing for the potential to be involved in binding, have many differences between the two isoforms, and are far from the catalytic domain, they were chosen as regions to test for binding affinity.

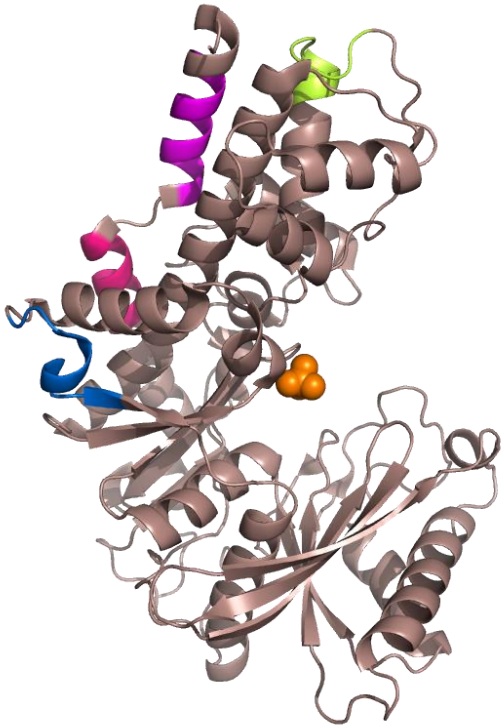

Figure 1. 6. *Saccharomyces cerevisiae* model with variant sites highlighted.
Model of *Saccharomyces cerevisiae* Hexokinase II highlighting swapped regions for creation of variant Hexokinase II (PDB 1IG8, (Kuser et al., 2000)). Four variants were produced by swapping out regions from Hexokinase I into Hexokinase II. The first variant is in magenta from amino

acids 25-34. Then the second is magenta and pink from amino acids 25-34 and 38-46. The third is in yellow from residues 321-329. The final variant is shown in blue and residues 443-452 were swapped. Image generated with PyMol.

1.7 Thesis objectives

The specific details of yHXK interactions with fungal VDAC are not understood and these are required for a better understanding of Hxk and VDAC interactions within yeast. To develop this understanding, this project had the following objectives:

i) to establish a procedure for over-expression of yeast hexokinases and variants for binding analysis

ii) to identify regions of Hxk1 that are candidates for determining binding specificity

ii) to characterize the enzymatic activities of the purified proteins and their variants

iii) to assess the binding of the purified variant proteins to ncVDAC

Chapter 2: Materials and Methods

2.1 Strains, Growth Conditions, Plasmids, and Reagents

Saccharomyces cerevisiae strain RY13 was used to produce hexokinase. The RY13 genotype is C13-ABYS-86 *MAT*α *pra*1-1 *prb*1-1 *prc*1-1 *cps*1-3 *ura*3Δ5 *leu*2-3, 112 *his*$^-$. The pESC$^-$ URA plasmid was cloned into RY13, and the plasmid contains the *URA*3 biosynthetic marker gene. The full native S*. cerevisiae* hexokinase I and hexokinase II were expressed with C-terminal his_6 tags; transcription occurred from the *GAL1* promoter on the pESC plasmid (Fig. 3.1). The expression strain was grown at 30°C. Synthetic complete medium with galactose as the sole carbon source (SD+Gal-Ura; 2.0 % (w/v) galactose, 1.7 % (w/v) yeast nitrogen base, 5 % (w/v) ammonium sulfate, 30 mg/L histidine, and 30 mg/L leucine) was used to grow the strain in order to induce transcription from the *GAL1* promoter of the pESC plasmid. Two plasmids, pESC-Hxk2-his_6-swap25-34 and pESC-Hxk2-his_6-swap319-328 were purchased from GenScript (Piscataway, NJ, USA) in which short sequences from Hxk1 were swapped into the Hxk2 gene (Fig. 1.6).

The purification of *N. crassa* VDAC (ncVDAC) was carried out via expression in *E. coli* c43. *E. coli* c43 was utilized due to being more resilient to the toxicity associated with overexpression (Dumon-Seignovert et al., 2004). The *N. crassa* VDAC gene was codon-optimized and cloned onto the pET21b vector using the NdeI and BamHI sites by GenScript; it was expressed with a C-terminal 6x his-tag (Fig. 3.7). *E. coli* BL21(c43) was used for expression and was grown in LB+Ampicillin (100 µg/mL) after transformation with pET21b vector (Ferens et al., 2019). *E. coli* was grown in liquid medium with shaking, at 37°C unless otherwise specified.

The detergent used to solubilize ncVDAC for MST experiments was n-decyl-β-d-maltopyranoside (DM, Anagrade, Maumee, OH, USA) and the cholesterol analogue was cholesteryl-hemisuccinate (CHS), which was purchased from Sigma-Aldrich Canada (Oakville, ON, Canada). AEBSF 4-(2-aminoethyl) benzenesulfonyl fluoride hydrochloride was used as a protease inhibitor for VDAC purifications. SigmaFAST Protease Inhibitor Cocktail Tablet, EDTA Free (AEBSF 2 mM, Phosphoramidon 1 µM, Bestatin 130 µM, E-64 14 µM, Leupeptin 1 µM, Aprotinin 0.2 µM, Pepstatin A 10 µM) was used for hexokinase protein purification (see below).

Protein Expression

2.2 VDAC Overexpression, Purification and Refolding

ncVDAC was overexpressed, purified, and folded as described in Ferens *et al*. (Ferens et al., 2019). A single *E. coli* Bl21(c43) colony containing pET21b-VDAC-his$_6$ was used to inoculate a 25-mL overnight culture of LB with ampicillin (100 µg/mL) medium, which was grown overnight. This culture was added to 500 mL of 37°C pre-warmed LB media to grow for 1 hour. At this point IPTG was added to a final concentration of 0.5 mM to induce VDAC expression; the culture was grown for 4 hours. Cells were harvested via centrifugation for 5 min at 8 000 rpm using a Sorvall SLA-3000 rotor. Cells were resuspended and chilled at 4°C in 30 mL of lysis buffer (20 mM Tris-Cl, 100 mM NaCl, 1 mM AEBSF pH 8.0). Cells were lysed via three passes through an EmulsiFlex C3 at 20, 000 psi. VDAC inclusions bodies were harvested from cell lysate by centrifugation at 16 000 rpm for 15 minutes in a Sorvall SS-34 rotor. The pellet containing the inclusion bodies was resuspended in 20 mM MOPS, 150 mM NaCl, 6 M guanidine-HCl and broken up using a glass Dounce homogenizer until no pellet was visible. The insoluble material

was removed by centrifugation at 20 000 rpm using a Sorvall SS-34 rotor. The supernatant was applied to 3 mL of Ni-NTA resin (Hispur^{TM} NI-NTA resin, Thermo Fisher Scientific, Winnipeg MB) and VDAC binding to the resin was done in batch with mixing for 2 hours at 4°C. After this the column was washed with 10 column volumes of 20 mM MOPS, 150 mM NaCl, 6 M guanidine-HCl followed by 4 column volumes of the same buffer with the addition of 20 mM imidazole. VDAC was eluted with 10 mL of 20 mM MOPS, 150 mM NaCl, 600 mM Imidazole, 6 M guanidine-HCl. Purified and denatured VDAC was then refolded by quickly diluting the protein solution 1/10 into 20 mM Tris-Cl, 300 mM NaCl, 1% DM, pH 8.0 and leaving it overnight to dialyse against 20 mM Tris, 300 mM NaCl, pH 8.0. The dialysis membrane had a molecular weight (MW) cut-off of 8 kDa. The ncVDAC sample was concentrated in a molecular weight concentrator with a 50 kDa cut off. Concentrated VDAC samples were loaded onto a 24 mL Superdex 200 increase column equilibrated with 20 mM MOPS, 100 mM NaCl, 0.3% DM, pH 7.0. to retrieve only non-aggregated protein. An additional run through the same column was performed with 20 mM MOPS, 100 mM NaCl, 0.3% DM, 0.06% CHS, pH 7.0 to introduce CHS into the sample. This sterol promotes oligomerization and induces VDAC into a more stable conformation that does not aggregate during MST testing with Hxk. In all cases a Superdex 200 increase column (GE Healthcare, Chicago, IL) was used to separate protein with a flow rate of 0.4 mL/min.

2.3 Hexokinase Overexpression and Purification

A single RY13 colony containing pESC^{-}URA3-Hxk-his$_6$ was used to inoculate a 15 mL-culture of synthetic defined medium (SD+Gal-Ura) with 2.0 % (w/v) galactose, 1.7 % (w/v) yeast nitrogen base, 5 % (w/v) ammonium sulfate, 30 mg/L histidine, and 30 mg/L of leucine. This strain was allowed to grow until it reached an OD_{600} of 2.0. Galactose was added in order to induce the transcription from the *GAL1* promoter of the pESC-URA plasmid. The entire culture was then used to inoculate 50 mL of SD+Gal-Ura and grown until it reached an OD of 2.0. At this point the entire culture was used to inoculate 1 L of yeast peptone galactose (YPGal) media with 2% galactose (w/v), 2% peptone (w/v), 1% yeast extract (w/v) and grown overnight. Lysis was carried out as described for *E. coli* except that the lysis buffer was 20 mM Tris-Cl, 150 mM NaCl, SigmaFAST Protease Inhibitor Cocktail Tablet, EDTA Free (AEBSF 2 mM, Phosphoramidon 1 µM, Bestatin 130 µM, E-64 14 µM, Leupeptin 1 µM, Aprotinin 0.2 µM, Pepstatin A 10 µM) pH 8. The cell lysate was centrifuged at 16,000 rpm in a Sorvall SS-34 rotor and the supernatant was applied to 3 mL Cobalt-NTA (Hispur^{TM} NI-NTA resin, Thermo Fisher Scientific, Winnipeg MB) resin to bind for an hour in batch. The column was washed with 10 column volumes of 20 mM Tris-Cl, 150 mM NaCl, pH 8.0. The VDAC column was then washed with 4 column volumes of 20 mM Tris-Cl, 150 mM NaCl, 20 mM Imidazole, pH 8.0. Then the hexokinase was eluted with 10 mL of 20 mM Tris-Cl, 150 mM NaCl, 300 mM imidazole, pH 8.0. Hexokinase was concentrated in a 30 kDa MW cut-off concentrator. Concentrated hexokinase samples of about 5 mg/mL were loaded onto a 24 mL Superdex 200 increase column equilibrated with 20 mM MOPS, 100 mM NaCl, pH 7.0. This was the running buffer required for the protein to be in for MST trials. In all

cases a Superdex 200 increase column was used to separate protein with a flow rate of 0.4 mL/min.

2.4 Hexose Kinase Assays

Saccharomyces cerevisiae has two isoforms of hexokinase both of which can phosphorylate glucose and fructose (Randez-Gil et al., 1998).

$$D-glucose+ATP \xrightarrow{HXK} glucose-6-P+ADP \text{ (2.1)}$$

$$D-fructose+ATP \xrightarrow{HXK} fructose-6-P+ADP \text{ (2.2)}$$

Assays were performed to determine the rate of phosphorylation of glucose and fructose for the two isoforms of hexokinase. Cuvettes were prepared with 50 mM Tris-Cl, 13.3 mM $MgCl_2$, 110 mM glucose, 82.5 nM ATP, 46.2 nM $NADP^+$, 1 U/mL Glucose-6-phosphate dehydrogenase, 0.5 mg/mL hexokinase. For the fructose kinase assay, the glucose was replaced with fructose, and 3 U/mL phosphoglucoisomerase was also added (Yamashita, 1988). This is a coupled reaction in which the second half is used to determine the rate.

$$glucose-6-P+NAD \xrightarrow{G6PD} gluconate-6-P+NADH+H^+ \text{ (1.3)}$$

Absorbance measurements were performed on a Ultrospec 3100 pro spectrophotometer. Absorbance at 340 nm was measured over 5 minutes immediately after hexokinase was added to determine the rate of phosphorylation by Hexokinase. Absorbance does not directly measure

hexokinase activity, and the coupled reaction is used to determine the rate of the reaction. The reduction of NAD^+ is the colorimetric portion of the assay, which causes a colour change that can be determined at an absorbance of 340 nm.

As per equation 2.4 only glucose can be used as a substrate for G6PD so phosphoglucoisomerase is required to convert fructose 6 -phosphate to glucose 6-phosphate.

$$glucose \overset{G6PI}{\longleftrightarrow} fructose \quad (2.4)$$

The specific activity of the enzyme is determined by the following calculation described by Worthington Biochemical Corporation (17).

$$\frac{Units}{\text{mg protein}} = \frac{\frac{\Delta A340}{\text{min}}}{6.22 \text{ x mg enzyme/mL reaction mixture}} \quad (2.5)$$

A unit refers to the amount of enzyme that catalyzes one micromole of phosphate addition to a hexose sugar per minute. A minimum of two technical replicates was used for all measurements.

Variants of yeast hexokinase II were tested and compared to the two wild-type enzymes. A ratio of the two specific activities was calculated to determine if any change to the specific phosphorylation activity for either hexose was impacted.

2.5 Microscale thermophoresis

Purified VDAC, post SEC is in solution with 20 mM MOPS, 100 mM NaCl, 0.3% DM, pH 7.0 and purified hexokinase is in 20 mM MOPS, 100 mM NaCl, pH 7.0. VDAC was labelled on lysine residues with Alexa fluor 647 NHS ester dye (Thermo-Fisher Canada, Mississauga, ON, Canada) according to the manufacturer's instructions. The protein was labeled so there was on average 1 label per protein molecule, as per the following equation:

$$\left(\frac{\mu g\ protein}{protein\ MW}\right)\ (1000)\ \left(\frac{molar\ ratio}{7.94}\right) = \ 2.31\ \mu L\ reactive\ dye\ to\ add\ to\ sample \quad (2.6)$$

The molar ratio for VDAC is 11. Then the dye was allowed to bind for 30 minutes in the dark. Afterwards the unbound dye was removed by centrifuging the dye through a resin as part of the Alexa fluor kit. Afterwards, VDAC was concentrated using a Amicon Ultra-4 Centrifugal Filter Unit with a 100 kDa MW cuttoff to 100 nM and hexokinase to 400 µM. Equal volumes of VDAC and hexokinase were mixed into standard capillaries from Nanotemper Technologies (München, Germany) to yield a final concentration of 50 nM VDAC. Hexokinase was added in 16 2-fold dilutions for measurement utilizing a Nanotemper Monolith NT.115. MST power was used at 20%.

We are only introducing two proteins and are therefore interested in bimolecular binding as described by the equation:

$$K_d = \frac{[A][B]}{[AB]} \quad (2.7)$$

K_d refers to the dissociation constant, [A] to the concentration of molecule A (VDAC), [B] to the concentration of molecule B (Hxk), and lastly [AB] is the concentration of the complex formed.

What is being measured through MST is the change in fluorescence in a localized area due to the movement of protein away from the source. A fluorescently tagged protein will move away from this area over time due to the heat of the laser. Therefore, the fluorescence after the localized heat source has warmed (F_{hot}) is measured relative to the fluorescence before the heat source was utilized (F_{cold}) and it is measured as:

$$F_n = \frac{F_{hot}}{F_{cold}} \cdot 1000 \quad (2.8)$$

F_n is the relative fluorescence of the sample. The fluorescently labeled partner is protein B and the unlabeled partner is protein A. The measured F_n of a sample composed of protein A, protein B, and complex AB is described by the equation:

$$F_n = \left(\frac{[B]}{B_{tot}}\right) + \left(\frac{[AB]}{B_{tot}} \cdot F_{AB}\right) \quad (2.9)$$

Where B_{tot} is the total concentration of component B (all bound and unbound), F_B is the F_n of protein B, and F_{AB} is the F_n of complex AB. The total concentration of proteins A and B can be described by the following equations:

$$A_{tot} = [A] + [AB] \quad (2.10)$$

$$B_{tot} = [B] + [AB] \quad (2.11)$$

Using equations 2.6 through 2.10 the F_n can be described as a function of A_{tot} which can be fit to a series of MST measurements at different A_{tot} values (usually a 2-fold serial dilution) to determine K_d:

$$F_n(A_{tot}) = F_B + \frac{(F_{AB} - F_B)\left(A_{tot} + B_{tot} + K_d - \sqrt{(A_{tot} + B_{tot} + K_d)^2 - (4A_{tot}B_{tot})}\right)}{2B_{tot}} \quad (2.12)$$

A_{tot} and B_{tot} are known concentrations equal to the total input concentration in an individual measurement. On the other hand, values for F_B, F_{AB}, and K_d will be determined by fitting the function to the experimental data if a full sigmodal binding curve is observed over all measured values of A_{tot} (Scheuermann et al., 2016). A more detailed explanation of the theory and analysis of MST data is presented by Scheuermann, et al., (2016)

Chapter 3: Results

3.1 Strategies for protein expression

Hxk and VDAC have been shown on numerous occasions to be binding partners in mammalian cells (Haloi et al., 2021). However, in yeast there seems to be little to no interaction between the two proteins under the conditions tested. Recently, Hxk1 has shown binding to ncVDAC (Ferens et al., 2019). Both hexokinase isoforms from *S. cerevisiae* were purchased and then separated and binding with only the Hxk1 isoform was determined via MST (Ferens et al., 2019). Because only Hxk1 showed a binding interaction to VDAC and Hxk2 did not, we wanted to determine if a specific region may be responsible. Yeast has two closely related isoforms of hexokinase HxkI and Hxk2. Hxk1 is 486 aa in length and yHxk2 is 487 aa in length and they are 77% identical at the amino acid sequence level. Most of the proteins is highly conserved, and a large portion of the unique amino acids are clustered in 3 regions, which are hypothesized to be responsible for the isoform-specific binding. Therefore, to determine which region may be responsible we wanted to create variants of Hxk2 that contained one of these regions as in HxkI. However, first we needed to develop a strategy to purify Hxk overexpressed in yeast cells and ensure Hxk1 binds and Hxk2 does not.

3.2 Hexokinase Purification

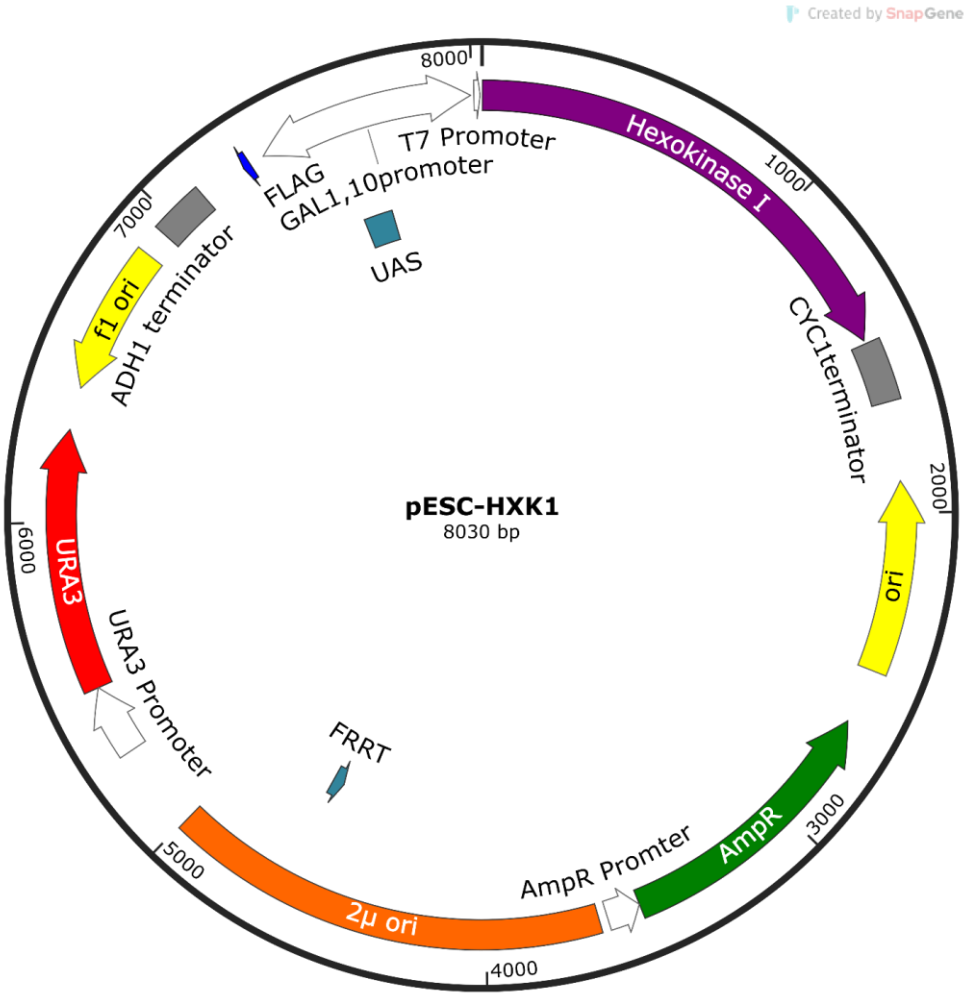

Figure 3. 1. pESC-URA3 shuttle vector

A diagram of the pESC-URA3 shuttle vector that has been utilized for the production of *S. cerevisiae* Hexokinase I and Hexokinase II. The Hexokinase genes were obtained from GenScript (N.J. U.S.) and were cloned in separate plasmids under the control of the *GAL*1,10 promoter and the *CYC*1 transcriptional terminator. The *HXK1* gene is shown here as an example. Replication in *S. cerevisiae* is driven by the origin of replication from the 2µ plasmid (2µ ori shown in dark

orange) and Ry13 cells containing the plasmid were selected using the *URA3* marker. The plasmid map was generated using SnapGene (https://www.snapgene.com/).

To examine the potential interaction between yeast hexokinase and VDAC, both proteins were overexpressed from a plasmid in an appropriate host. Purification of hexokinase could have potentially been achieved in a few different hosts. *E. coli* was a potential host of choice to produce hexokinase due to the ease of producing large quantities of protein. Several different *E. coli* strains (RIL and T7 (this thesis), DH5α and C43 (F. Ferens personal communication) were attempted; however, even though protein could be produced in some strains, high levels of aggregation and other anomalies were observed (protein seemed to exist in larger oligomeric forms based on SEC (Size exclusion chromatography) data). Since *E. coli* appeared to be non-viable yeast was used instead. The added benefit of using *S. cerevisiae* is that we were producing *S. cerevisiae* hexokinase which is its native protein. Yeast is capable of proper phosphorylation and other post translational modification of a eukaryotic protein.

For the production of hexokinase 1 and hexokinase 2, the pESC plasmid (Fig. 3.1) was utilized. The key selective feature in this plasmid is *URA3* (in red), that completements the *ura3-52* mutation in the host strain Ry13. This is a very stable biosynthetic selection method. The transcription of the hexokinase gene (in purple) is under the control of the Galactose 1, 10 promoters (GAL in white). Since production of hexokinase is under the control of the *GAL* promoter in the pESC plasmid, galactose media had to be used to induce its production. First the cells were grown in minimal media in the presence of glucose as to not induce the production of hexokinase as the cell OD was increasing. Then only after a large mass of cells was produced the cells were centrifuged and added to YPGal media. Complex media

was used for the final day of growth to make the cells as healthy and metabolically active as possible to produce higher amounts of hexokinase. However, the transition between glucose and galactose metabolism provided very inconsistent results and delayed growth. To resolve this galactose was used for the entirety of the growth phase. Firstly, cells were grown in minimal galactose media to retain the plasmid until an OD of 1.0. Then the cells were transferred to YPGal for a day to grow until an OD of 3.0. Following induction of hexokinase, the EmulsiFlex C3 was utilized to lyse the yeast cells. SigmaFAST Protease Inhibitor Cocktail Tablet was added to prevent protease activity. The EmulsiFlex provides the ability to continuously lyse a large volume of cells. This is ideal since for *S. cerevisiae* Ry13 because a large volume of cells which was required to obtain enough protein. After the cells were ruptured, they were centrifuged and hexokinase is a water-soluble protein that exists in the cytosolic space, and therefore, will exist in the supernatant.

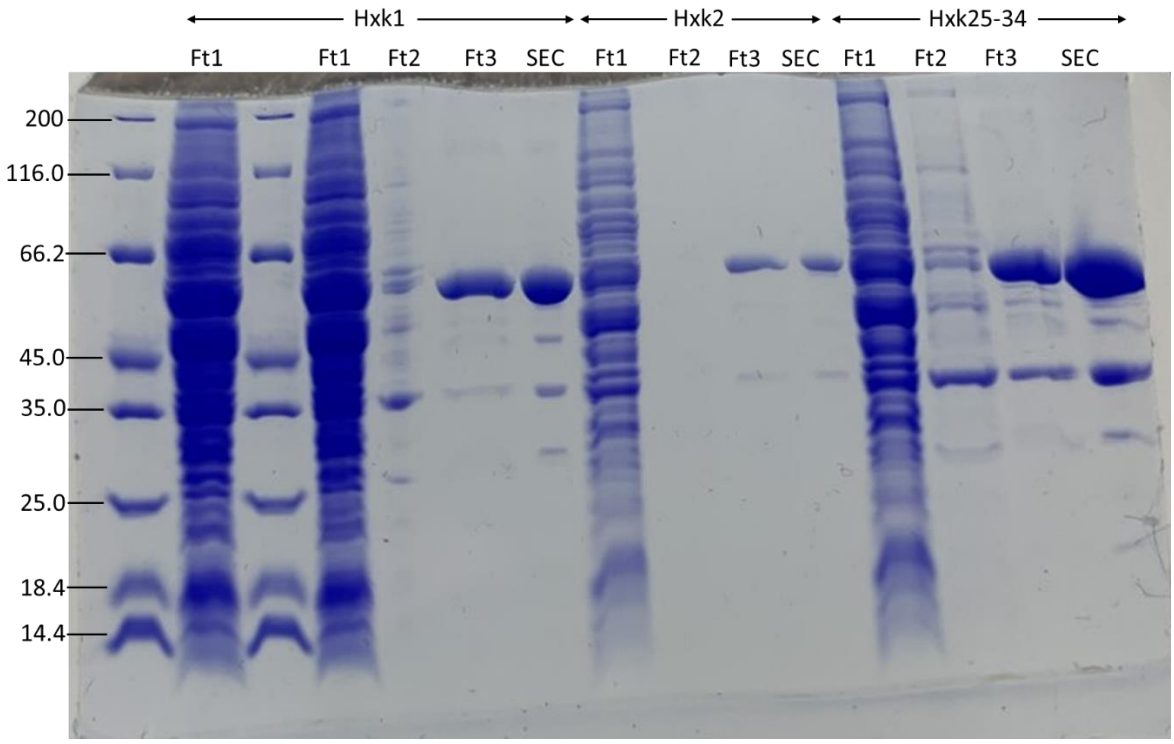

Figure 3. 2. SDS-PAGE of hexokinase (1)

SDS-PAGE analysis of fractions of Hexokinase purification. Samples were run through a 12% SDS-PAGE gel and stained with Coomassie blue. FT1 is the sample collected during the first wash, FT2 during the second wash, FT3 is the elution out of the Ni-NTA agarose column. SEC is a sample from the pooled fractions from the Hexokinase monomer and dimer peak eluted from molecular size-exclusion chromatography Superdex 200 increase column. Yeast Hexokinase is 55 kDa in size.

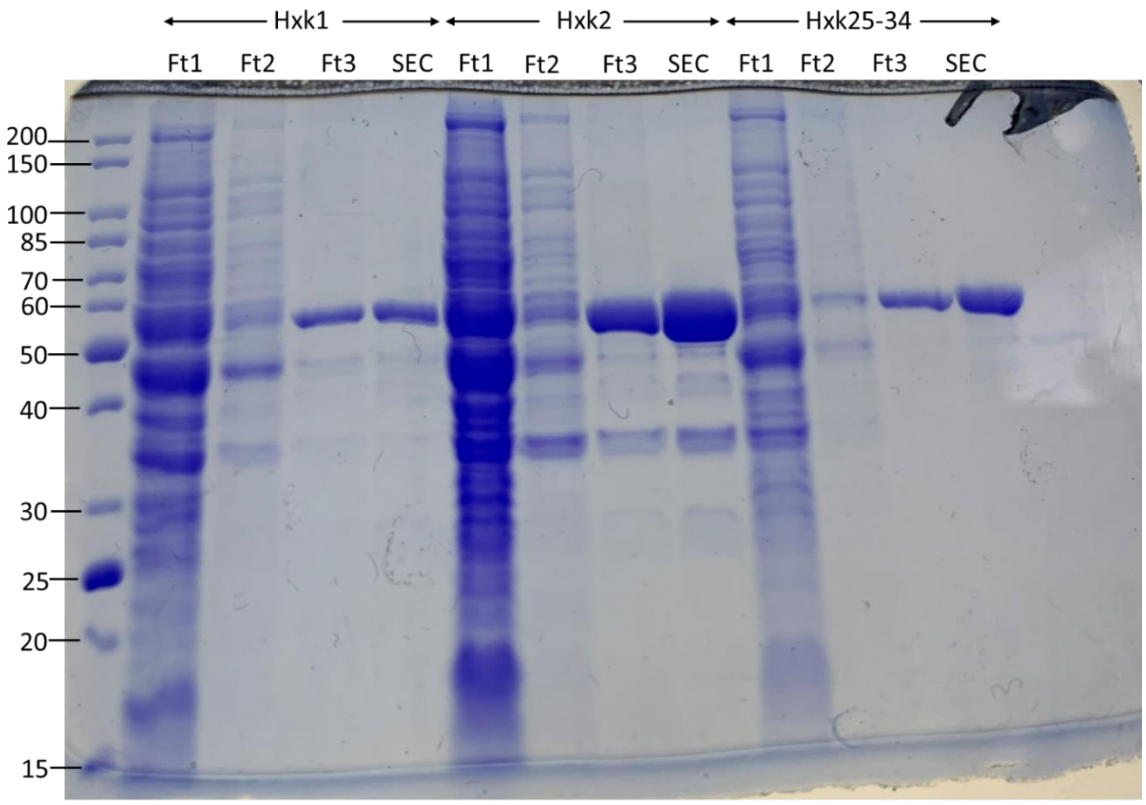

Figure 3. 3. SDS-PAGE of hexokinase (2)

SDS-PAGE analysis of fractions of Hexokinase purification. Samples were run through a 12% SDS-PAGE gel and stained with Coomassie blue. FT1 is the sample collected during the first wash, FT2 during the second wash, FT3 is the elution out of the Ni-NTA agarose column. SEC is a sample from the pooled fractions from the Hexokinase monomer and dimer peak eluted from molecular size-exclusion chromatography Superdex 200 increase column. Yeast Hexokinase is 55 kDa in size.

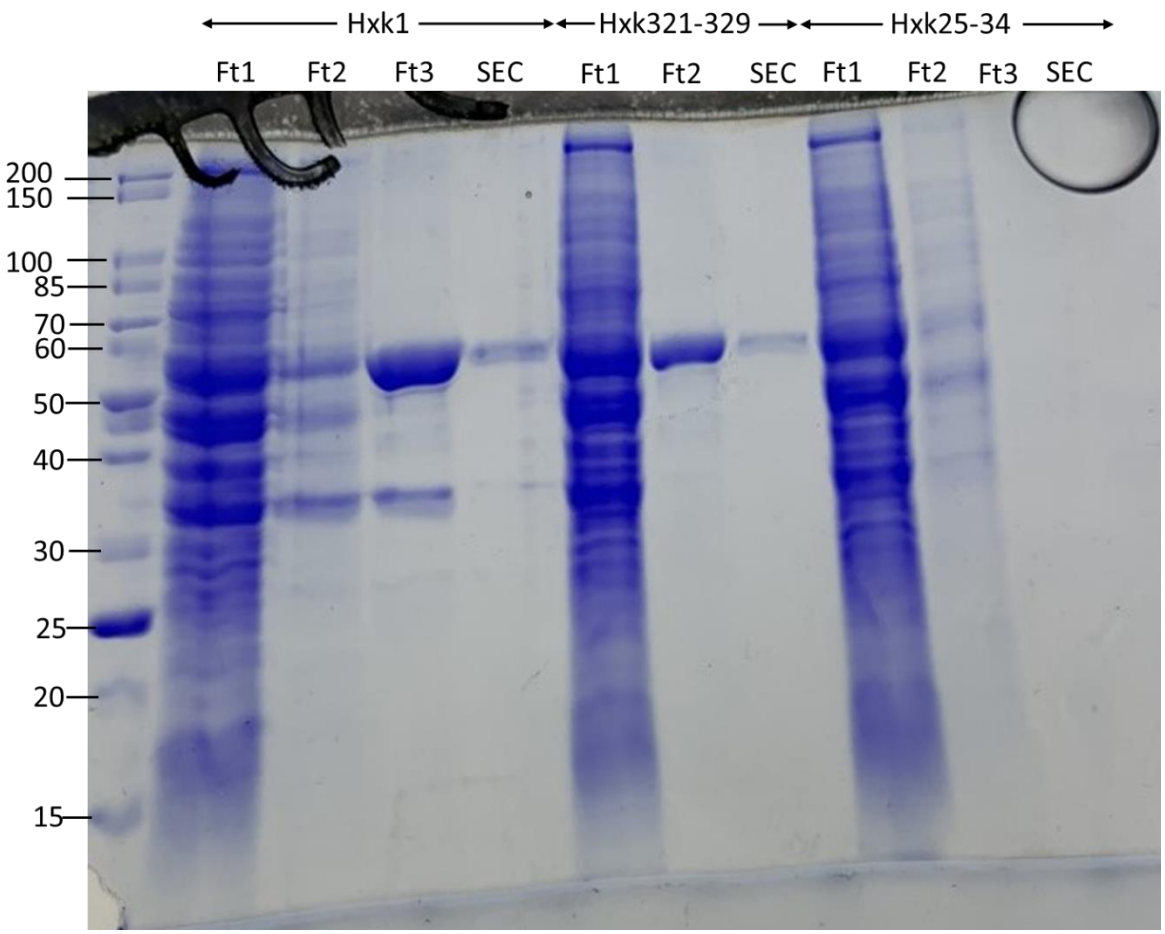

Figure 3. 4. SDS-PAGE of hexokinase (3)

SDS-PAGE analysis of fractions of Hexokinase purification. Samples were run through a 12% SDS-PAGE gel and stained with Coomassie blue. FT1 is the sample collected during the first wash, FT2 during the second wash, FT3 is the elution out of the Ni-NTA agarose column. SEC is a sample from the pooled fractions from the Hexokinase monomer and dimer peak eluted from molecular size-exclusion chromatography Superdex 200 increase column. Yeast Hexokinase is 55 kDa in size.

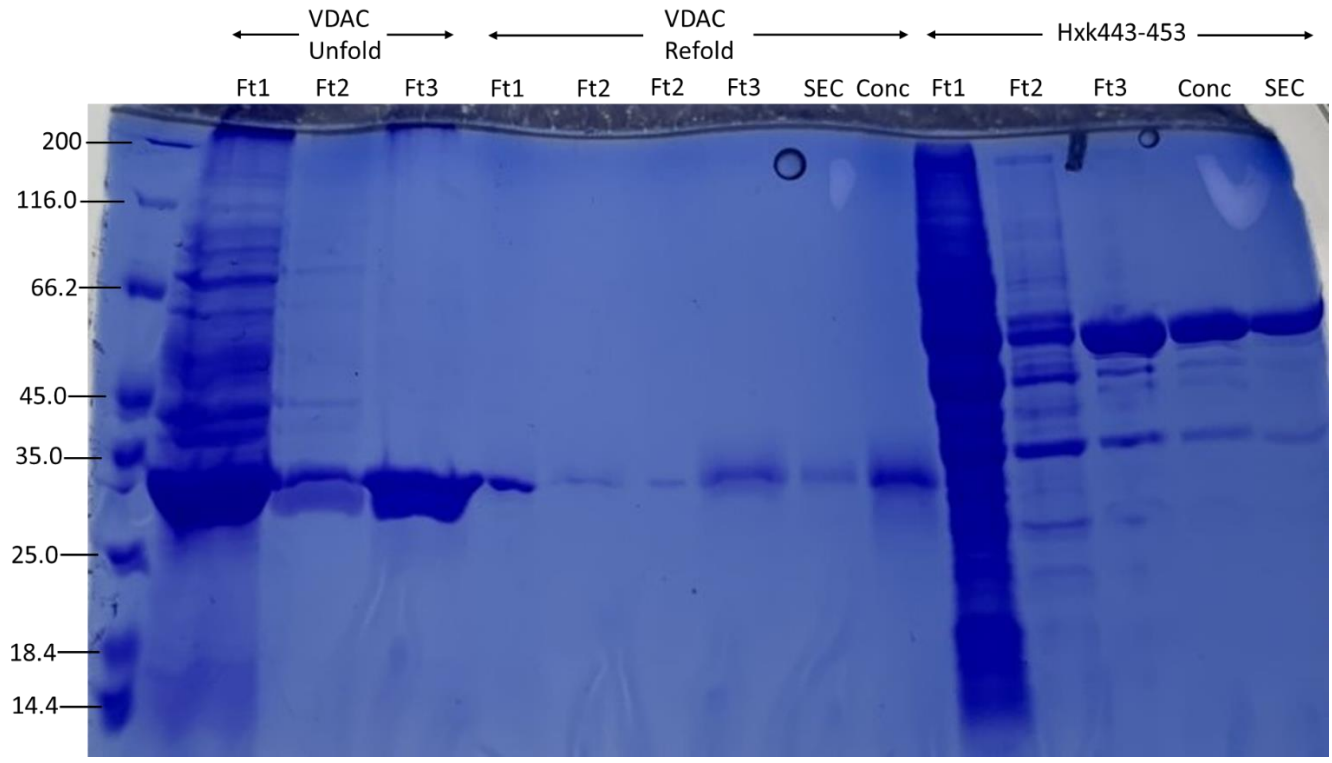

Figure 3. 5. SDS-PAGE of hexokinase and VDAC

SDS-PAGE analysis of fractions of Hexokinase purification. Samples were run through a 12% SDS-PAGE gel and stained with Coomassie blue. FT1 is the sample collected during the first wash, FT2 during the second wash, FT3 is the elution out of the Ni-NTA agarose column. SEC is a sample from the pooled fractions from the Hexokinase monomer and dimer peak eluted from molecular size-exclusion chromatography Superdex 200 increase column. Yeast Hexokinase is 55 kDa in size. VDAC (voltage dependent anion channel) unfold is when the protein is completely denatured. VDAC refold is after the protein has been refolded in a detergent micelle.

After separating the supernatant from the cell debris, the protein was purified from the supernatant. All purified proteins contain a His_6 tag which is used to purify the protein of interest. The supernatant was mixed for an hour with Ni-NTA agarose at 4°C to prevent degradation. At the end of binding the mixture was run through a column constituting the first wash phase. Then a second wash phase with 20 mM imidazole was performed to wash off any weakly bound proteins. Then hexokinase was eluted from the column using 300 mM imidazole. Reasonably pure protein is accomplished at this point as seen with SDS-PAGE gel electrophoresis (Figures 3.2-3.5). Hexokinase is 55 kDa and some minor bands can be viewed that are constant across samples and both wildtype hexokinase variants. Any cleaved hexokinase that contains the His_6 portion of protein will still be purified.

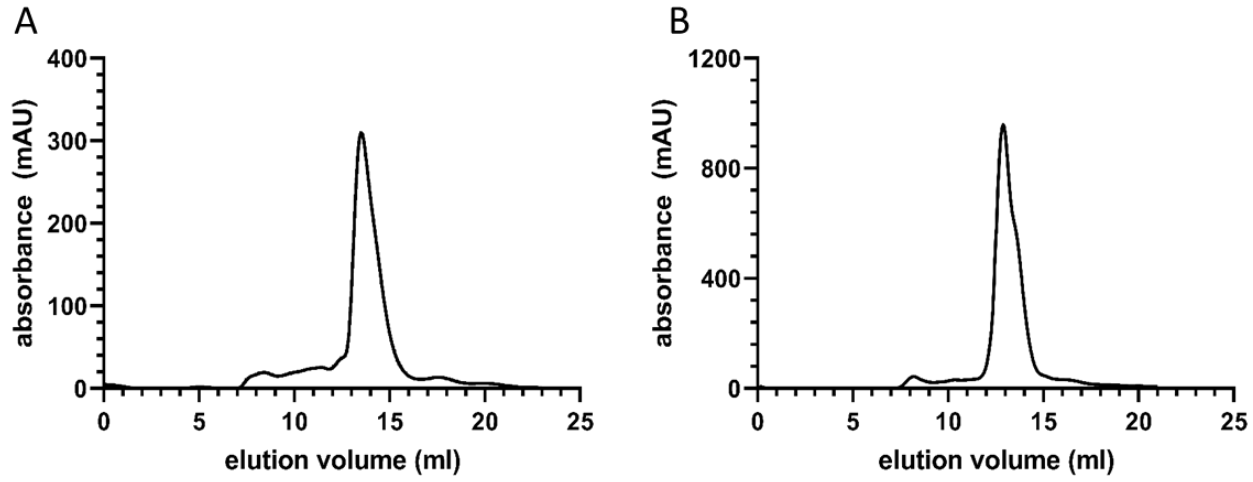

Figure 3. 6. Molecular size-exclusion chromatography for hexokinase 1 and 2.
Molecular size-exclusion chromatography (SEC). Hexokinase eluted in fractions through a Superdex 200 increase column (GE Healthcare) with 20 mM MOPS, 100 mM NaCl, pH 7.0 buffer at a flow rate of 0.4 mL/min. The volume of protein injected was 1 mL total. (A) Hexokinase I

dimer eluted at 13 mL and monomer at 14 mL. The monomer shoulder is not noticeable, but in a large majority SEC runs of Hxk1 it is more clearly distinguished. (B) Hexokinase II dimer eluted at 12.5 mL and monomer at 13.5 mL.

Purified hexokinase was concentrated in a molecular weight concentrator with a 50 kDa cut off and loaded onto a 24 mL Superdex 200 increase column (Fig. 3.6). Hxk I dimer eluted at 13 mL and monomer at 14 mL. Hxk2 dimer eluted at 12.5 mL and monomer at 13.5 mL. The proportion of dimer was also higher for Hxk2 than for Hxk1. Some minor bands can still be visualized via SDS-PAGE in the monomer and dimer hexokinase fractions after size exclusion chromatography.

3.3 VDAC Purification

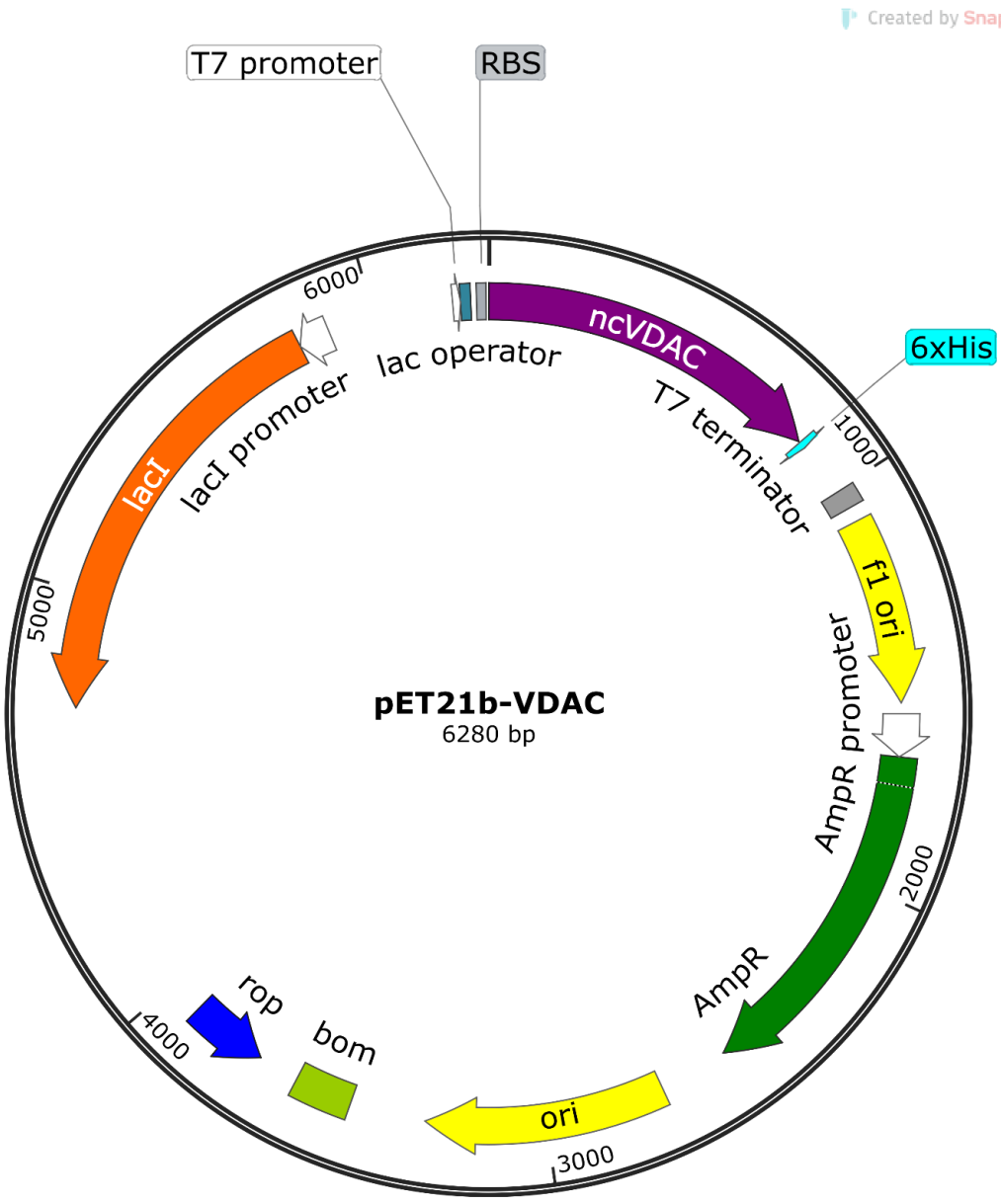

Figure 3. 7. pET21b plasmid

A diagram of pET21b plasmid that was utilized for the production of *Neurospora crassa* VDAC (ncVDAC) in C43 *E. coli*. Expression of ncVDAC is controlled by a lac operator that, in the presence of lactose or an analog, is not bound by LacI, allowing the T7 promoter to bind and

transcribe the ncVDAC gene. ncVDAC will be synthesized with a 6xHis tag on the C terminal end. The plasmid map was generated using SnapGene.

Voltage dependent anion channel (VDAC) is a mitochondrial outer membrane (MOM) protein. Unlike hexokinase that can be purified and stable in a standard aqueous state a membrane protein requires additional components. For the production of VDAC the pET21b plasmid (Fig. 3.7) was utilized within *E. coli* C43. In order to select for this plasmid, ampicillin resistance resulting from the expression of the AmpR gene (green) was used. LacI (orange), the repressor, is continually expressed to prevent the production of ncVDAC. ncVDAC is a non-native protein to *E. coli* and will be unfolded and packed within inclusion bodies. Therefore, it is beneficial to limit ncVDAC production until a large cell density can be achieved. Then the allolactose analog IPTG was used to induce transcription of ncVDAC from the *lac* operator. The EmulsiFlex C3 was used to disrupt the cell membranes physically. The lysed cells were centrifuged and, the cell pellet was kept as ncVDAC is contained in inclusion bodies instead of being water soluble. At this point a glass homogenizer was used to break up all of the cell debris to release ncVDAC into solution. Then another round of centrifugation was utilized to remove all of the cell debris. ncVDAC could be improperly folded however, 6M guanidine-HCl is used to ensure we start from a completely unfolded starting point. The solution was then mixed and bound with Ni-NTA agarose for 2 hours. The column was then washed with 10 column volumes of 6 M guanidine-HCl containing buffer (Unfolded Ft1, Fig 3.5 and Fig 3.9) followed by 4 column volumes of the same buffer with the addition of 20 mM imidazole (Unfolded Ft2, Fig 3.5 and Fig

3.9). The second wash step ensures any poorly bound protein will elute. Then ncVDAC was eluted with 10 mL 600 mM Imidazole and 6 M guanidine-HCl (Unfolded Ft3, Fig 3.5 and Fig 3.9).

Purified recombinant denatured VDAC was then refolded by quickly diluting the protein solution 1/10 into buffer containing 1% n-decyl-β-d-maltopyranoside (DM) and no guanidine-HCl, pH 8.0 and leaving it overnight to dialyse against the same buffer without DM. The dialysis membrane had a molecular weight (MW) cut-off of 8 kDa. These conditions allow for the refolding of ncVDAC into a detergent micelle. The dialysis membrane allows for the slow removal of guanidine-HCl. The refolded VDAC solution was then mixed with Ni-NTA agarose for an hour. For the washing and elution of the column no guanidine-HCl is used and, DM was used in all solutions. First the column was washed with 10 column volumes without imidazole (Folded Ft1, Fig 3.5 and Fig 3.9), then washed with 4 column volumes with 20 mM imidazole (Folded Ft2, Fig 3.5 and Fig 3.9). Afterwards, 10 mL of solution with 300 mM imidazole was used to elute refolded VDAC (Folded Ft3, Fig 3.5 and Fig 3.9).

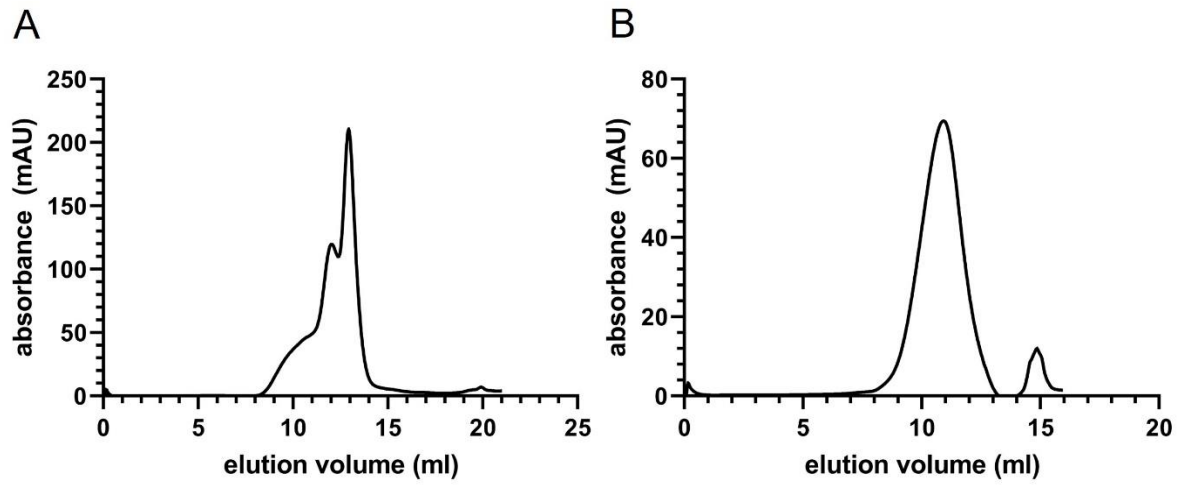

Figure 3. 8. Molecular size-exclusion chromatography for VDAC.

Molecular size-exclusion chromatography (SEC). Voltage dependent anion channel (VDAC) eluted in fractions through a Superdex 200 increase column (GE Healthcare). The volume of protein injected was 0.5 mL total. (A) Buffer with 20 mM MOPS, 100 mM NaCl, 0.3% n-Decyl-β-D-maltopyranoside (DM), and pH 7.0 at a flow rate of 0.4 mL/min. (B) Buffer with 20 mM MOPS, 100 mM NaCl, 0.3% DM, 0.06% Cholesteryl-hemisuccinate (CHS) and pH 7.0 at a flow rate of 0.4 mL/min. DM is a detergent and CHS is a sterol and in the presence of CHS VDAC has a wider and earlier peak with less monomers and more larger oligomers.

VDAC was concentrated and loaded onto a 24 mL Superdex 200 increase column (Fig. 3.8). The column was run with a solution with 0.3% DM (Fig. 3.8 A). DM is a detergent that is needed for VDAC remain in solution within the micelle and detergent has low fluorescence so to limit this the concentration used is lower than that to refold. Then a second SEC run for VDAC is completed using a solution with 0.3% DM and 0.06% Cholesteryl-hemisuccinate (CHS) (Fig. 3.8 B). CHS is a sterol that will exist within the detergent micelle and alter the average oligomeric conformation of VDAC to be in larger oligomers. Under this state VDAC was able to bind Hxk1 and not Hxk2 using purchased Hxk (Ferens 2019).

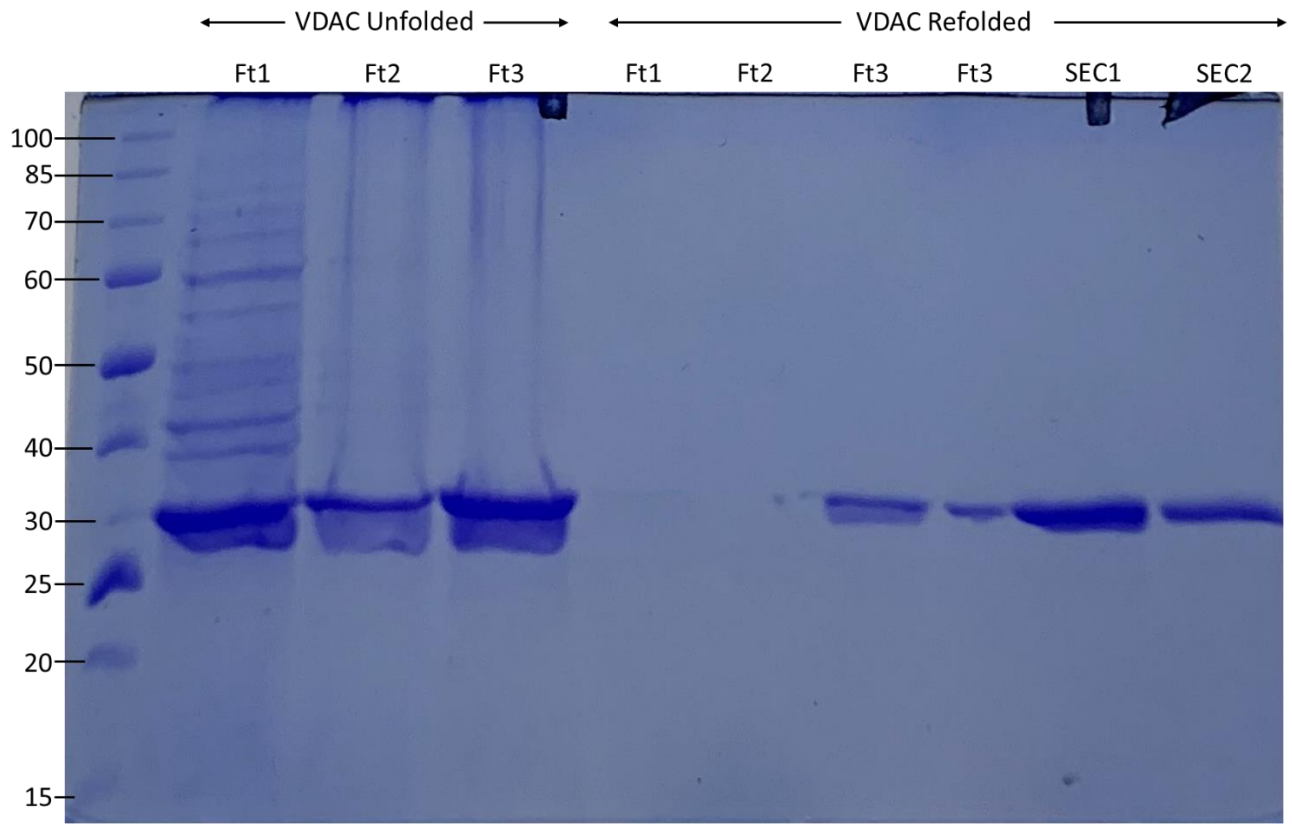

Figure 3. 9. SDS-PAGE for VDAC.

SDS-PAGE analysis of VDAC purification. Samples were run through a 12% SDS-PAGE gel and stained with Coomassie blue. FT1 is the sample collected during the first wash, FT2 during the second wash, FT3 is the elution out of the Ni-NTA agarose column. SEC is a sample from the pooled fractions from the Hexokinase monomer and dimer peak eluted from molecular size-exclusion chromatography Superdex 200 increase column. ncVDAC is 30 kDa.

The SDS-PAGE Gel shows that very pure protein is obtained (Fig. 3.9). VDAC is about 30 kDa which can be viewed in the unfolded and refolded samples. Unfolded VDAC elutes in the wash and elution fractions. This suggests that a high percentage of the protein is not binding to

the Ni-NTA resin. It is possible that when produced in *E. coli* and purified from inclusion bodies the protein is sometimes aggregated, potentially preventing the His_6 tag from being bound. The unfolded VDAC fraction that eluted in imidazole was kept and refolded. With this refolded VDAC sample no protein elutes in the first two fractions. This suggests that very little protein is aggregated, and the His_6 tag is available for binding. There was no change in the migration of VDAC on the SDS-PAGE gel after the addition of sterol. Once both Hxk isoforms and VDAC were purified we used MST to determine if there was an interaction as seen with the commercial sample of Hxk (Ferens 2019).

3.4 Microscale Thermophoresis for Wildtype Hexokinase

In order to determine binding interaction between hexokinase and VDAC after they were both purified one member of the binding pair needed to be labeled. Alexa fluor 647 NHS ester dye was utilized to covalently bind approximately 1 molecule of dye per molecule of protein. After labeling is completed, VDAC was diluted to 100 nM. Hexokinase was concentrated to 400 µM and then 16 2-fold serial dilutions were performed. The labeled protein concentration (VDAC) was held constant for all 16 samples, so any difference is due to the presence of a certain concentration of hexokinase. In MST VDAC fluorescence changes over time as VDAC moves and if hexokinase concentration affects this movement, it will affect the change in fluorescence over time.

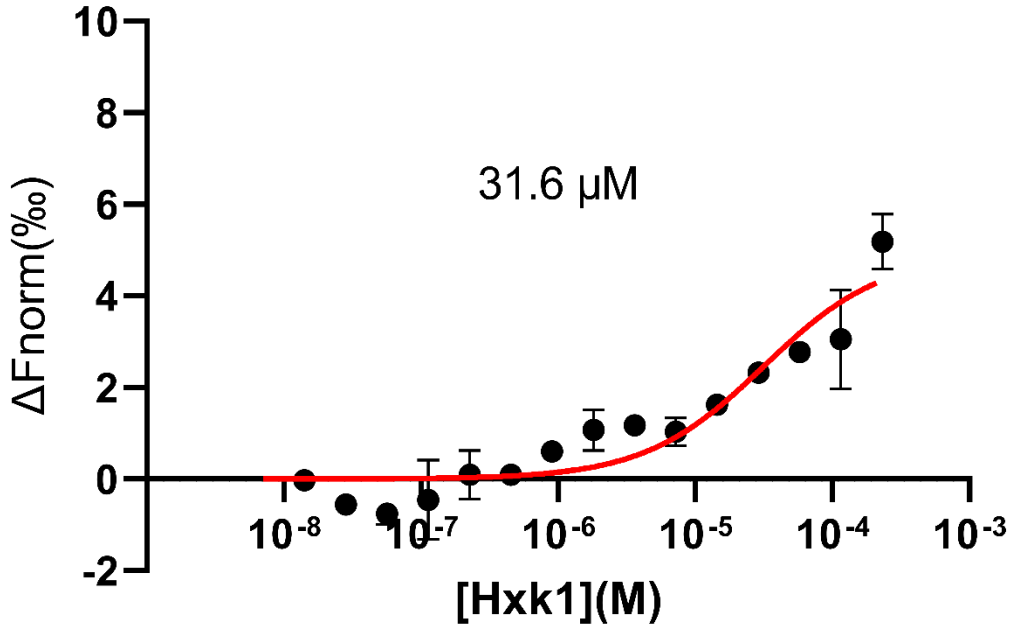

Figure 3. 10. Microscale thermophoresis for VDAC-Hxk1.

Titration of unlabeled Hxk1 against a constant concentration of fluorescently labelled VDAC. Delta normalized fluorescence represents the change in fluorescence after 5 seconds with the background fluorescence removed. The K_d of the interaction and the fitted curve (red) used to determine the K_d are shown on the plot. Nanotemper Monolith NT. 115 was used for MST data acquisition and the data was graphed using GraphPad Prism.

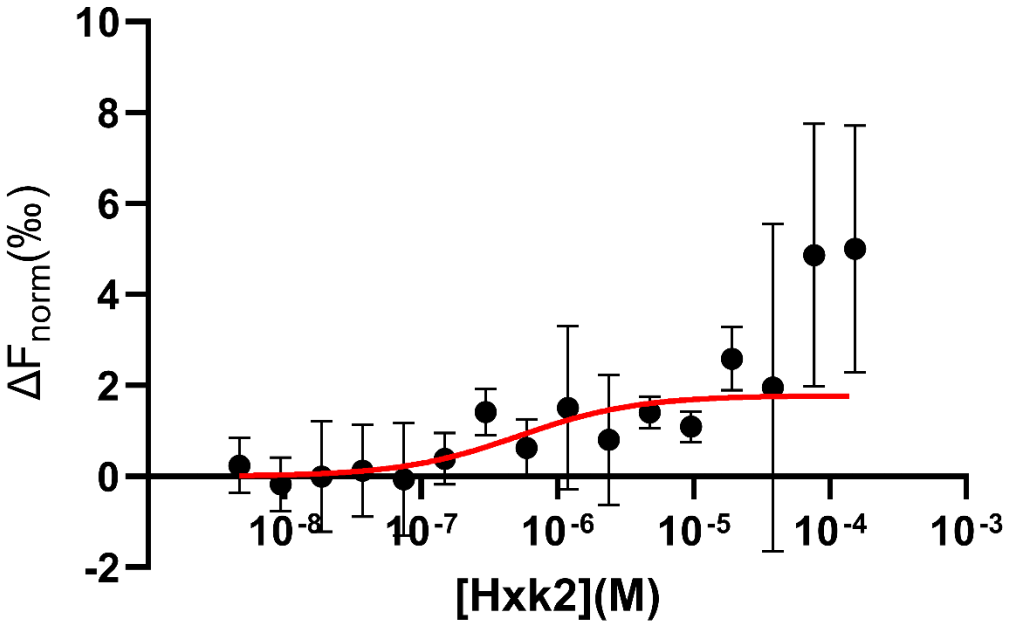

.

Figure 3. 11. Microscale thermophoresis for VDAC-Hxk2.

Titration of unlabeled Hxk2 against a constant concentration of fluorescently labelled VDAC. Delta normalized fluorescence represents the change in fluorescence after 5 seconds with the background fluorescence removed. The K_d of the interaction and the fitted curve (red) used to determine the K_d are shown on the plot. Nanotemper Monolith NT. 115 was used for MST data acquisition and the data was graphed using GraphPad Prism.

A binding constant for ncVDAC+Hxk1 of 31.6 +/- 15.6 µM was determined (Fig. 3.10), whereas the other wildtype isoform Hxk2 did not bind to ncVDAC (Fig. 3.11). When comparing the two wildtype isoforms for Hxk2 the binding constant does not even clear the background response amplitude. Therefore, since the noise appears to be as great as the binding constant there is no reason to assume binding as occurred. However, for Hxk1 weak binding seems to

exist. Hxk1 has a binding coefficient of 31.6 µM which is weak; however, it is noticeably different and stronger than the Hxk2 isoform. This replicates the data from Ferens 2019 of 27 ± 6 µM, indicating that the in-house purified hexokinases have the same properties as the commercially available ones.

3.5 Hexokinase II Variants Creation, Purification, and MST

	Amino Acids 25-34
Hxk1 aa sequence	DEIHQLEDMF
aa contrast	+I E +F
Hxk2 aa sequence	QQIENFEKIF
	Amino Acids 25-48
Hxk1 aa sequence	DEIHQLEDMFTVDSETLRKVVKHF
aa contrast	+I E +FTV +ETL+ V KHF
Hxk2 aa sequence	QQIENFEKIFTVPTETLQAVTKHF
	Amino Acids 321-329
Hxk1 aa sequence	LNEKGLMLK
aa contrast	+ ++G + K
Hxk2 aa sequence	MYKQGFIFK
	Amino Acids 443-451
Hxk1 aa sequence	GDASKD-PI
aa contrast	+ D PI
Hxk2 aa sequence	QTSLDDYPI

Figure 3. 12. Sequences of *S. cerevisiae* used to create mutants.

Segments from a *S. cerevisiae* hexokinase I and hexokinase II alignment. Hexokinases I and II are 77% identical at an amino acid level and these regions cluster a high percentage of the unique

amino acids. An empty space means there are different amino acids in the alignment and a + refers to a similar amino acid.

S. cerevisiae Hxk1 and Hxk2 are 77% similar at the amino acid level and most of these differences are concentrated within the non-catalytic or regulatory regions (Kuser 2008). Therefore, some region or regions is likely responsible for the isoform specific binding to VDAC**.** Hxk1 and hxk2 in *S. cerevisiae* amino acid sequences were aligned to determine where the two proteins were unique (Fig. 3.12). Most of the unique amino acids were clustered into a few regions.

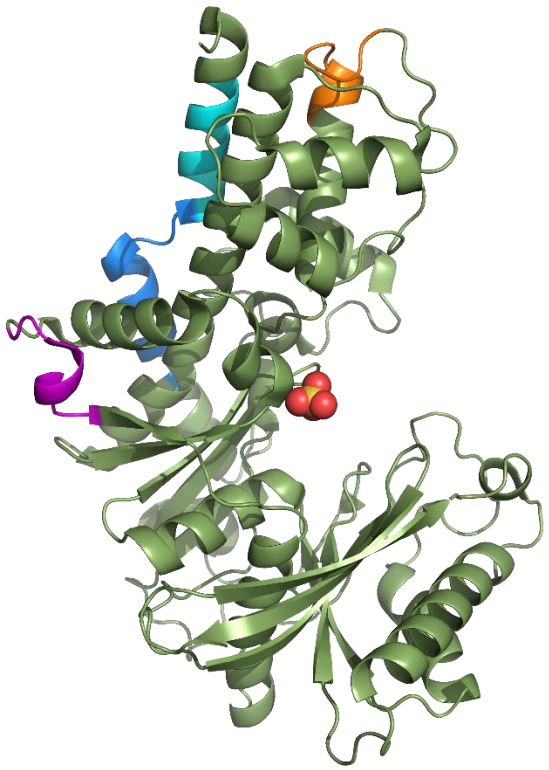

Figure 3. 13. Hexokinase II model with mutation locations highlighted.

PyMOL generated structure of *Saccharomyces cerevisiae* hexokinase II using the crystal structure (1IG8 PDB, (Kuser et al., 2000)). The red and yellow ball structure in the center is SO4 and it represents the catalytic binding site. The four coloured sections along the protein represent the locations selected for making hexokinase I variants. The variant sections based on amino acid sequence are, teal (25-34), teal and blue (25-48), orange (321-329), purple (443-452).

Also, both proteins have been previously crystallized, and the catalytic domain has been determined. Using this information, the catalytic region as well as the regions that are internal to the protein were not considered as candidates for interaction with VDAC. Four variants were created based upon the regions that are expected to be on the surface away from the catalytic site and therefore potentially involved in binding interactions. The chosen regions are also in the clustered regions with many amino acid derivations between the isozymes. Coding sequences for segments of *Hxk1* were swapped into *Hxk2* in the same plasmids as the wildtypes. A model was created to show the four variants of Hxk2 (Fig. 3.13). The teal section is swapped for the Hxk25-34 variant, the teal and blue section is swapped for the Hxk25-48 variant, the orange section is swapped for the Hxk321-329 variant, and the purple section is swapped for the Hxk443-452 variant. The red and yellow molecule in the open space is SO_4 and it is at the catalytic site.

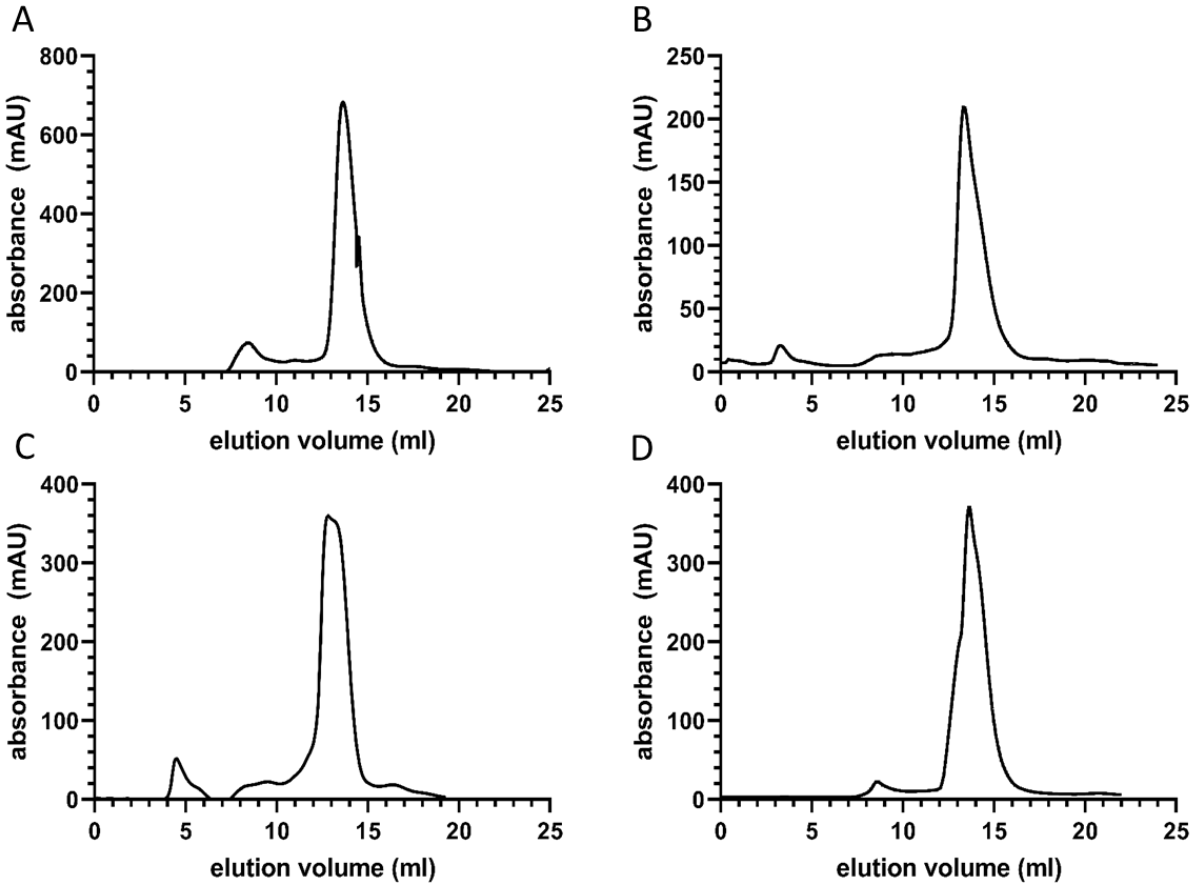

Figure 3. 14. Molecular size-exclusion chromatography for Hxk2 variants.

Molecular size-exclusion chromatography (SEC). Hexokinase eluted in fractions through a Superdex 200 increase column (GE healthcare) with 20 mM MOPS, 100 mM NaCl, pH 7.0 buffer at a flow rate of 0.4 mL/min. The volume of protein injected was 1 mL total. (A) Hexokinase25-34 dimer eluted at 13 mL and monomer at 14.5 mL. (B) Hexokinase25-48 dimer eluted at 13 mL and monomer at 14 mL. (C) Hexokinase321-329 dimer eluted at 12.5 mL and monomer at 13 mL. (D) Hexokinase443-452 dimer eluted at 13 mL and monomer at 14 mL.

All hexokinase variants were produced and purified in the same manner as the wildtype proteins. Hexokinase variants are also 55 kDa just like the wildtype isoforms. Likewise, they also

show the same minor bands (Fig. 3.2, Fig. 3.3, Fig. 3.4). When it comes to SEC the monomer and dimer elution points of the wildtype isoforms and the Hxk2 variants are all very similar (Fig. 3.14). The elution volumes for the dimers are between 12.5 and 13 mL, whereas the elution volumes for the monomers are between 13 and 14.5 mL.

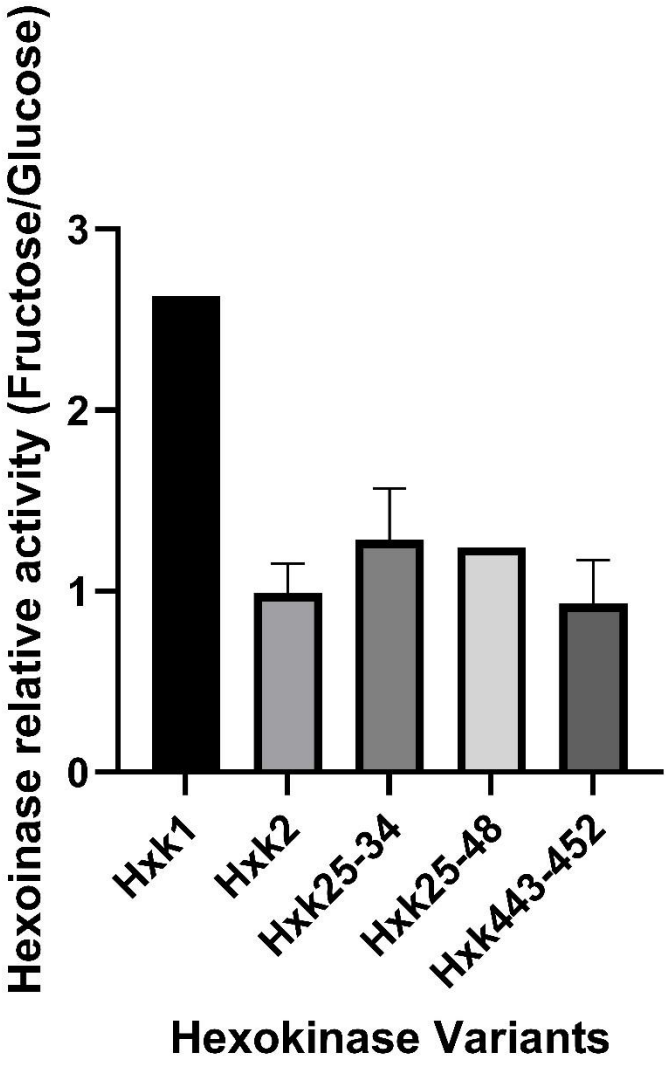

Figure 3. 15. Relative hexokinase activity on fructose and glucose.

Relative hexokinase activity on fructose and glucose. An indirect assay was used to measure kinase activity of the two wild-type (Hxk1 and Hxk2), and three Hxk2 variants were measured on fructose and glucose. The average ratio of activity (fructose/glucose) is presented, along with standard deviations. The three variants are Hxk2 in which amino acids of a specific region were swapped with those present in the Hxk1 isoform (see figure 3.12). n = 3 for Hxk2 and Hxk25-34, Hxk1 and Hxk25-48 had n = 1, and Hxk443-452 had n = 2. A one-way ANOVA with the Tukey test was done for Hxk2 and Hxk25-34, and the difference is non-significant (ns).

Hexokinase is an enzyme capable of phosphorylating several different hexose sugars. Yeast hexokinase 1 has a higher specific activity for fructose than hexokinase 2. Hexokinase 1 in *S. cerevisiae* has a fructose/glucose relative activity of 2.5-3, whereas, Hexokinase 2 has a fructose/glucose relative activity of 1.3 (Banuelos et al., 1977; Berthels et al., 2008; Kuser et al., 2008). The ratios of activity on fructose and glucose were assessed instead of specific activities because each individual preparation varied in purity. The ratios are a stable measurement between protein preparations.

Based on their position in the three-dimensional structure of the protein (Fig. 3.13.), the amino acid replacements in the three Hxk2 variants were not predicted to alter the active site. Therefore, the relative activities on fructose and glucose were expected to be similar to those of the wild-type Hxk2. The Hxk25-34 variant had a relative activity ratio of 1.28, the Hxk25-48 variant had a ratio of 1.24, and the Hxk443-452 had a ratio of 0.93 (Fig. 3.15). They fall within a range very similar to their wildtype isoform Hxk2 and very dissimilar to the wildtype Hxk1 isoform. Further replicates are needed to provide statistical support for the similarities among

the activities of Hxk25-34, Hxk443-452, and Hxk2. Nonetheless, this data suggest that the replacements did not affect the catalytic function significantly.

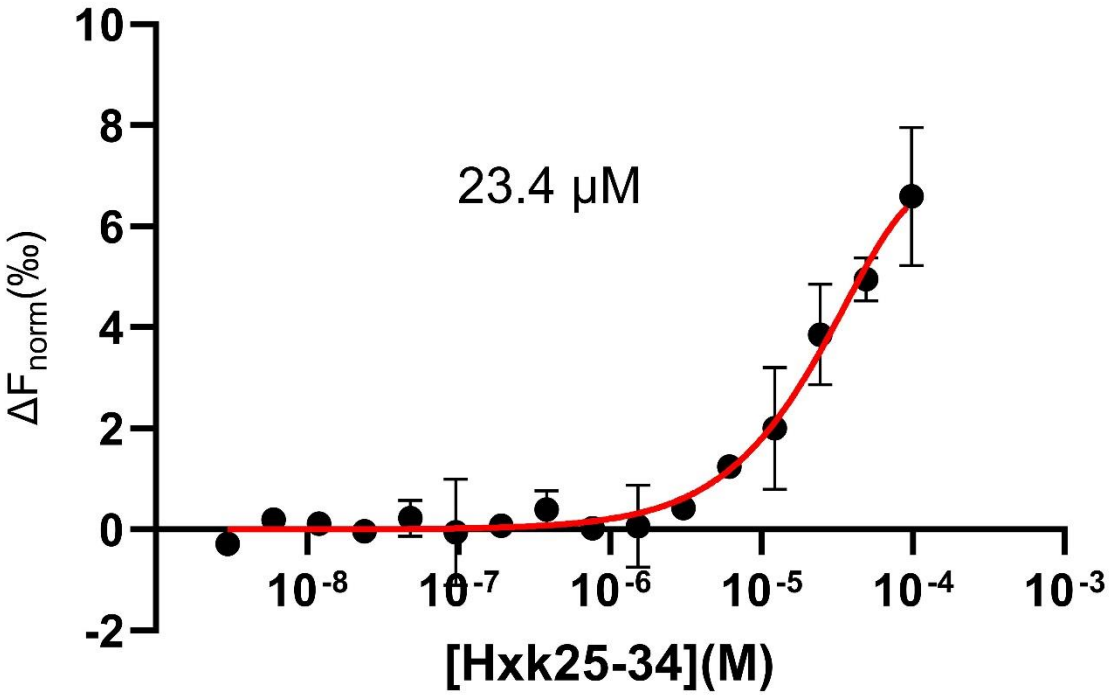

Figure 3. 16. Microscale thermophoresis for VDAC-Hxk25-34.
Titration of unlabeled Hxk2swap25-34 against a constant concentration of fluorescently labelled VDAC. Delta normalized fluorescence represents the change in fluorescence after 5 seconds with the background fluorescence removed. The K_d of the interaction and the fitted curve (red) used to determine the K_d are shown on the plot.

After it was determined that the four Hxk2 variants were folded and functional we used MST to determine if any variants may either partially or fully confer Hxk1-like binding to VDAC. Protein preparation and MST were completed with the identical procedure used for the

wildtype isoforms. A binding constant for ncVDAC + Hxk2swap25-34 of 23.4 +/- 19.0 µM was determined (Fig. 3.16.). This suggests gain of function for binding affinity can be accomplished by replacing amino acids 25 through 34 in the yHxk2 isoform. It is possible that more is required to impart the same binding affinity that exists in Hxk1. Either another segment or elongating the 25-34 amino acid swapped segment could be necessary to fully impart Hxk1-like interaction with VDAC. However, Hxk25-34 shows a similar binding affinity for ncVDAC to that of the Hxk1 isoform that had a Kd of 31.6 +/- 15.6 µM. Analysis of further replicates is needed to accurately determine the relative strengths. Also, testing the other Hxk2 variants may be required to better elucidate the binding interaction, especially the 25-48 variant.

Chapter 4: Discussion

This research sought to determine the regions involved with the isoform-specific binding of Hxk to VDAC. The data in this thesis indicate that the replacement of residues 25-34 with those from Hkx1 seems to have mostly to fully conferred the ability for weak or transient binding of Hxk2 to VDAC. Hxk1 has a binding affinity of 31.6 +/- 15.6 and Hxk25-34 has a binding affinity of 23.4 +/- 19.0. The binding affinity are of the same order of magnitude, which suggest that this region is likely mostly responsible for binding to VDAC. However, it is possible that additional sequences are required to impart the same binding affinity that exists for Hxk1. Either a separate segment or the entire region of difference (25-48) that includes the 25-34 amino acid swapped segment (Fig. 3.13) could be necessary to fully impart a Hxk1-like interaction with VDAC. Testing the other Hxk2 variants is required to better elucidate the binding interaction, of particular interest is the 25-48 variant. Once the regions of importance are determined, single amino-acid swaps to Hxk2 could be used to determine which residues are involved in binding. It is likely that one of the residues contributing to the negative charge in amino acids 25-34 that exists in the binding isoform is the most likely candidate (Fig. 4.1).

A secondary method to confirm the MST results would also be invaluable. Co-IP (Co-Immunoprecipitation), pull-down assays, crosslinking protein interaction analysis, label transfer protein interaction analysis, and far-western blot analysis are all potential methods to determine confirm Hxk-VDAC interactions. Each of these different approaches is most appropriate for a different range of protein interactional strength. The binding interaction between yeast Hexokinase and ncVDAC is very weak according to the data obtained via MST. This seems reasonable because the N-terminal anchor that seems primarily responsible for

binding in mammals does not exist in the yeast versions of hexokinase (Fig. 1.3 (Haloi et al., 2021; Ma et al., 1989; Randez-Gil et al., 1998)). Nonetheless, greater than 80% of proteins do exist in a complex of some form, and weak or transient interactions can be determined with some methods (Rao 2014). Many methods such as Co-IP and pull-down assays are very specific and only strong interactions will be selected for, making them less appropriate for future studies. Co-IP was already attempted between Hxk1 and VDAC with a negative result (data not shown). Only one experiment was run as of yet, but it is likely this method will not yield results for weak binding. Therefore, a method that allows for the determination of weak interactions such as crosslinking protein interaction analysis could be used.

Covalently crosslinking can link together proteins that are only briefly or transiently interacting, so they can be studied. Pull down experiments in cell extracts allow for native proteins to be tested in native conditions, even with membrane proteins (Berggard et al., 2007; Rao et al., 2014). However, *in* vivo crosslinking is hard to control and cell lysis must be done so proteins with weak interactions tend not to yield results so this approach will not likely work (Berggard et al., 2007; Rao et al., 2014). Therefore, using a hydrophilic crosslinker with purified hexokinase and VDAC in a detergent micelle could work. If hexokinase is interacting with VDAC from the cytosolic side of the mitochondrial outer membrane, it would be an exposed portion of VDAC that hexokinase is interacting with and a hydrophilic crosslinker should be required. After crosslinking, another method is required to analyze the bound products. Western blot or Immunoprecipitation (IP) with anti-VDAC antibodies, or Mass Spectrometry of the crosslinked products could be used to determine if protein interaction did occur (Horney et al., 2001; Rao

et al., 2014). Since the MST data showed that Hxk1 bound VDAC and Hxk2 did not, excessive crosslinking leading to any false positives would be readily apparent.

Label transfer protein interaction analysis (Horney et al., 2001; Neely et al., 2002; Rao et al., 2014) could be done instead of standard crosslinking. Label transfer is a method in which a photoactive, and potentially biotinylated crosslinker is covalently bound to a purified bait protein (Horney et al., 2001; Neely et al., 2002). Then the bait protein is mixed with a protein that may potentially be able to bind the bait protein (Horney et al., 2001; Neely et al., 2002). After allowing time for the reaction UV light is used to active the crosslinker causing it to react with the prey protein (Neely et al., 2002). After the reaction, the crosslinker is cleaved from the original bait protein (Neely et al., 2002). At this point either the prey or nothing will be attached to the crosslinker. The crosslinker, which contains a label such as biotin, can be used for purification and detection of the prey protein. Western blot or mass spectroscopy can be used to identify the prey protein (Neely et al., 2002).

The results indicate that residues 25-34 are important in the VDAC-Hxk1 interaction. To learn more about this region and how it might be involved in binding, these areas were modeled for vacuum electrostatics and hydrophobicity (Fig. 4.1 and Fig. 4.2). Both isoforms have known crystal structures to model after (Kuser et al., 2008; Kuser et al., 2000). The PDB files for both isoforms were imported into PyMOL (Schrödinger, 2023). Then the sequence of the Hxk2 isoform was changed in the 25-34 amino acid region to swap the residues to those present in the Hxk1 isoform. A protein contact potential representation was done to show surface electrostatics for all three version of the protein (Fig. 4.1). Hxk2 is much more neutral in the 25-34 region, whereas both Hxk1 and Hxk25-34 are negative. This suggests the negative

charge in this region may be vital to allow binding to VDAC. The Hxk25-34 swap variant is very similar in point charge throughout the circled region to Hxk1 (Fig. 4.1). Also, the electrostatic potential of Hxk25-34 is mostly similar to that of Hxk1, not its parent isoform. All three molecule files were then analyzed in ChimeraX for hydrophobicity (Fig. 4.2). Hydrophobicity for the 25-34 region among the three variants is not very distinct except for one region. The very top of the models there is a hydrophilic region in both Hxk1 and Hxk2-25-34 and a hydrophobic region in Hxk2. The electrostatic and hydrophobicity changes in the 25-34 region are likely responsible for why they are capable of weak or transient binding with VDAC and Hxk2 is not. Also, the knowledge that this region is negatively charged and hydrophilic means that the binding surface in VDAC likely will be hydrophilic and positively charged.

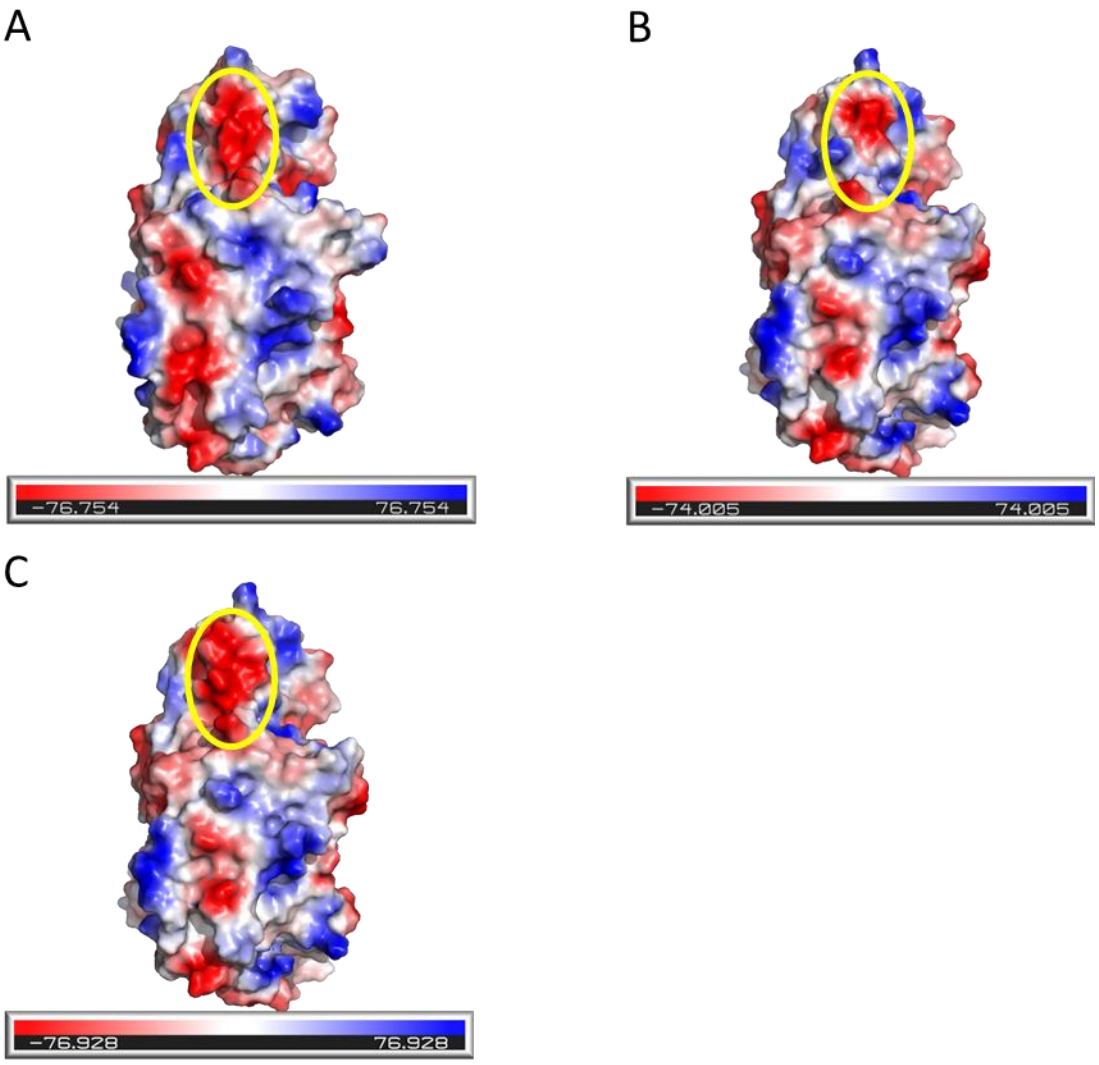

Figure 4. 1. Hexokinase surface electrostatics models.

Hexokinase surface electrostatics generated using PyMOL. (A) Hxk1 generated based upon crystal structure (3B8A PDB, (Kuser et al., 2008)). (B) Hxk2 generated based upon crystal structure (1IG8 PDB, (Kuser et al., 2000)). (C) Hxk25-34 generated based upon crystal structure and then mutated using PyMOL (1IG8 PDB).

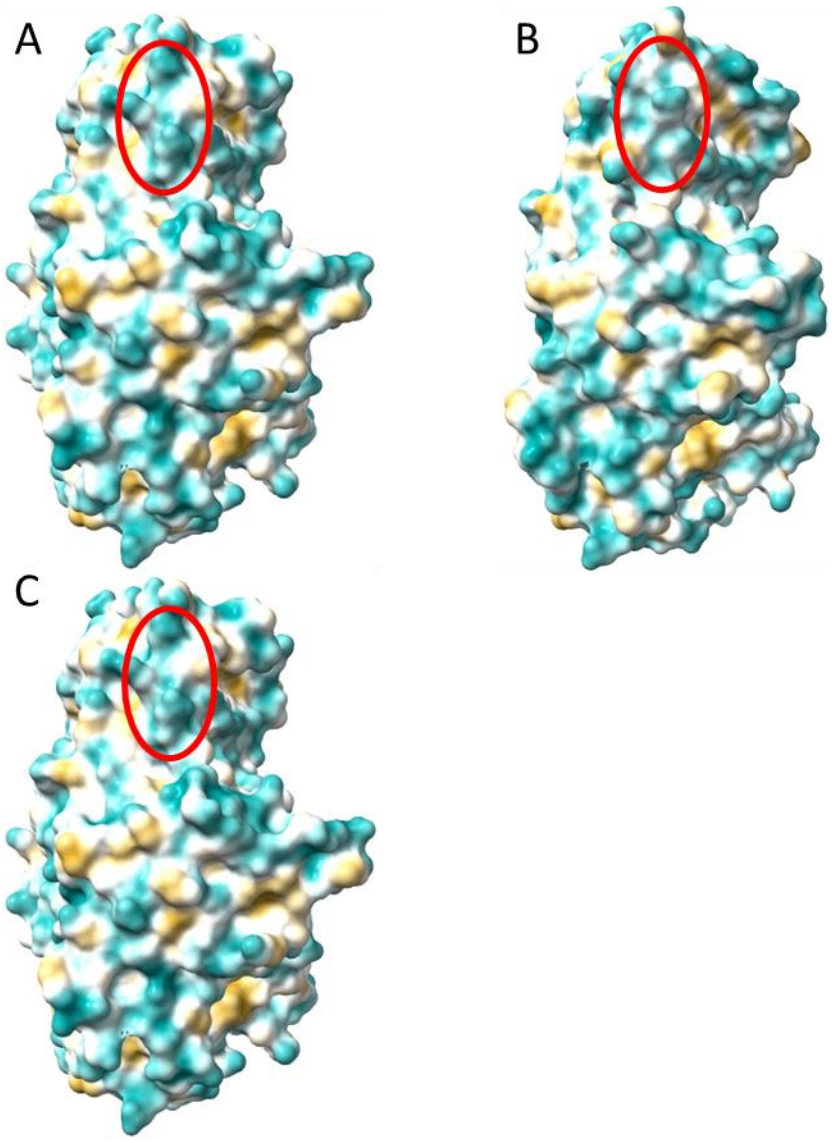

Figure 4. 2. Hexokinase surface polarity models.

Hexokinase surface polarity generated using ChimeraX (Meng et al., 2023) dark cyan is more hydrophilic and yellow, white is neutral, and yellow is hydrophobic. (A) Hxk1 generated based upon crystal structure (3B8A PDB, (Kuser et al., 2008)). (B) Hxk2 generated based upon crystal structure (1IG8 PDB, (Kuser et al., 2000)). (C) Hxk25-34 generated based upon crystal structure of Hxk2 and then mutated using PyMOL (1IG8 PDB, (Kuser et al., 2000)).

After confirmation of Hxk1 and VDAC binding, as well as the determination of the location(s) of Hxk1 that is required for the binding, the next step is to determine what portion of VDAC it is interacting with. As a membrane protein a large segment of VDAC is non-accessible for Hxk interaction. VDAC exists as 19 transmembrane β-strands and a N-terminal α-helix (Bayrhuber et al., 2008; Hiller et al., 2008; Ujwal et al., 2008). The amino acid region from 25-34 in Hxk2 that was mutated is hydrophilic and negatively charged (Fig. 4.1 and Fig. 4.2). Potentially, the same workflow using MST could be utilized by mutating the VDAC loops in the hydrophilic and positively charged portions. There are several positively charged regions predicted on the surface of VDAC (Bay et al., 2012), Fig 4.3) that could interact with the negatively charged 25-34 region. Multiple glycine or alanine can be used to replace the entire loop, or a hydrophilic portion of the loop, or single lysine or arginine residues can be substituted by glycine or alanine. Changes that prevent the Hxk1 and VDAC interaction must be the region responsible for binding. Another possible method would be to use crosslinking mass spectrometry (Piersimoni et al., 2022). Hxk and VDAC would be crosslinked, and then mass spectrometry data could be analyzed to determined where in the protein was crosslinked to determine where in VDAC is responsible for binding (Piersimoni et al., 2022).

The research in Ferens et al. 2019 and in this thesis advance the field of VDAC-Hxk interactions. Previously, it was examined if VDAC and hexokinase bound each other. The majority of experiments seemed to suggest that there was no interaction between yeast hexokinase and VDAC (Aflalo & Azoulay, 1998; Forte et al., 1987; Kovac et al., 1986). The general literature consensus was that fungal hexokinase and VDAC did not bind since they could not co-recover hexokinase with mitochondria purification (Pastorino & Hoek, 2008).

Mammalian hexokinase on the other hand across a number of species have been found to bind VDAC (Mazure, 2017; Shoshan-Barmatz et al., 2020). This difference can be partially explained by the fact that the mammalian version of hexokinase 2 has an N-terminal α-helix that was found to be responsible for binding; it is not present in the fungal version (Fig. 1.3). However, the lack of the N-terminal α-helix does not preclude weak or transient interactions with VDAC mediated by other sites in the protein, and therefore, the lack of hexokinase binding to mitochondria in the early experiments is not unexpected. Since Hxk1 does appear to bind to VDAC weakly, this potentially leads to the reopening of VDAC and hexokinase research in fungal systems. These are key proteins when it comes to metabolism and regulation and the proteins interacting leads to new avenues of study.

Hxk in yeast is known to be critical in a large regulatory process known as carbon catabolite repression (CCR, (Schmidt et al., 2020). CCR is a regulatory process in which, in the presence of glucose, alternative carbon sources are not required, and the associated genes are blocked from transcription (Schmidt et al., 2020; Vega et al., 2016). Hxk2 has been shown to be involved in CCR but the regulatory regions of Hxk involved are still unknown (Schmidt et al., 2020; Vega et al., 2016). Hxk2 creates a large complex with Mig1 and Mig2, binding the *SUC2* promoter region and preventing transcription of the gene (Fernandez-Garcia et al., 2012; Schmidt et al., 2020; Vega et al., 2016). It is Hxk2 and not Hxk1 that is involved in this complex. Therefore, the differences in their regulatory regions may have a number of impacts on interaction including CCR. The Hxk2 swap variants created for this thesis can be used to screen for Mig1 binding, like the wildtype isoform.

Better understanding of the impact hexokinase has on CCR could be extremely important because this appears to be linked to *Candida albicans* (Ca) ability to be pathogenic to humans (Laurian et al., 2019). Hexokinase has a wide array of regulatory impacts that generally improve its fitness in areas from metabolic flexibility to aiding with stress such as hypoxia (Laurian et al., 2019). The CaHxk2 hexokinase, was determined to be in the nucleus where in other fungi it is known to interact with the Mig complex for CCR (Laurian et al., 2019). Null mutants of CaHxk2 or mutants in both glucokinases are hypovirulent. Even when CaHxk2 is complemented the percent survival is still vastly increased (Laurian et al., 2019). Learning more about this regulatory process and the regions involved could help in understanding this opportunistic pathogen and other fungal human pathogens.

In summary, the work in this thesis confirms the binding of fungal hexokinase to VDAC and reveals important information about the contact sites in Hxk1, thereby forming the basis for future studies into this important area of fungal biochemistry.

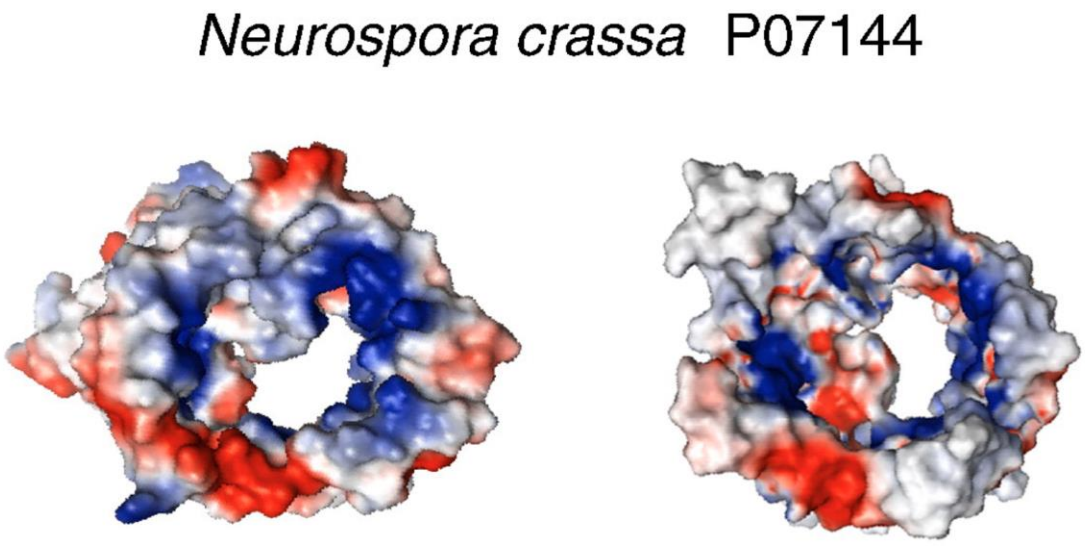

Figure 4. 3. Electrostatic model of *N. crassa* VDAC.

Electrostatic model of the two faces of *N. crassa* VDAC using PyMol. Edited from Bay et al. 2012 with permission. Blue regions are positively charged and red regions are negatively charged.

Chapter 5: Conclusions

In this research microscale thermophoresis was used to analyze ncVDAC and yeast Hxk binding affinity. This yielded the following conclusions:

1) Hxk1 is capable of weak binding interactions with ncVDAC and Hxk2 is not.
2) The Hxk25-34 variant is capable of weak binding interactions with ncVDAC.
3) All of the hexokinase variants were capable of hexokinase activity similar to their parent isoform.

The re-examination of fungal Hxk-VDAC interaction provides potentially valuable and interesting new avenue of study. VDAC and hexokinase are both critical proteins for cell regulation, growth, and survival; therefore, better understanding their impact on fungal cell regulation is valuable. The results not only provide insight into fungal VDAC-Hxk interactions but reopen wider areas of investigation that were ruled out by some earlier research. The Hxk25-34 variant of Hxk2 was shown to be able to gain binding affinity to ncVDAC suggesting this approach could work for hexokinase interaction analysis in other yeasts. For example, CCR has been shown to be linked to virulence in *Candida albicans* and thus, investigating VDAC-hexokinase interactions and their isoform specificity could provide further insight into this opportunistic human pathogen (Laurian et al., 2019; Vega et al., 2016). Lastly, determining the region(s) of VDAC required for binding to hexokinase in fungi is critical to understanding the interactions between these two important regulatory proteins.

Chapter 6: References

Aflalo, C., & Azoulay, H. (1998, Jun). Binding of rat brain hexokinase to recombinant yeast mitochondria: effect of environmental factors and the source of porin. *J Bioenerg Biomembr, 30*(3), 245-255. https://doi.org/10.1023/a:1020544803475

Arzoine, L., Zilberberg, N., Ben-Romano, R., & Shoshan-Barmatz, V. (2009, Feb 6). Voltage-dependent anion channel 1-based peptides interact with hexokinase to prevent its anti-apoptotic activity. *J Biol Chem, 284*(6), 3946-3955. https://doi.org/10.1074/jbc.M803614200

Banuelos, M., Gancedo, C., & Gancedo, J. M. (1977, Sep 25). Activation by phosphate of yeast phosphofructokinase. *J Biol Chem, 252*(18), 6394-6398. https://www.ncbi.nlm.nih.gov/pubmed/19473

Bay, D. C., Hafez, M., Young, M. J., & Court, D. A. (2012, Jun). Phylogenetic and coevolutionary analysis of the beta-barrel protein family comprised of mitochondrial porin (VDAC) and Tom40. *Biochim Biophys Acta, 1818*(6), 1502-1519. https://doi.org/10.1016/j.bbamem.2011.11.027

Bayrhuber, M., Meins, T., Habeck, M., Becker, S., Giller, K., Villinger, S., Vonrhein, C., Griesinger, C., Zweckstetter, M., & Zeth, K. (2008, Oct 7). Structure of the human voltage-dependent anion channel. *Proc Natl Acad Sci U S A, 105*(40), 15370-15375. https://doi.org/10.1073/pnas.0808115105

Berggard, T., Linse, S., & James, P. (2007, Aug). Methods for the detection and analysis of protein-protein interactions. *Proteomics, 7*(16), 2833-2842. https://doi.org/10.1002/pmic.200700131

Berman, H. M., Westbrook, J., Feng, Z., Gilliland, G., Bhat, T. N., Weissig, H., Shindyalov, I. N., & Bourne, P. E. (2000, Jan 1). The Protein Data Bank. *Nucleic Acids Res, 28*(1), 235-242. https://doi.org/10.1093/nar/28.1.235

Berthels, N. J., Cordero Otero, R. R., Bauer, F. F., Pretorius, I. S., & Thevelein, J. M. (2008, Jan). Correlation between glucose/fructose discrepancy and hexokinase kinetic properties in different Saccharomyces cerevisiae wine yeast strains. *Appl Microbiol Biotechnol, 77*(5), 1083-1091. https://doi.org/10.1007/s00253-007-1231-2

Dumon-Seignovert, L., Cariot, G., & Vuillard, L. (2004, Sep). The toxicity of recombinant proteins in Escherichia coli: a comparison of overexpression in BL21(DE3), C41(DE3), and C43(DE3). *Protein Expr Purif, 37*(1), 203-206. https://doi.org/10.1016/j.pep.2004.04.025

Easterby, J. S., & Rosemeyer, M. A. (1972, Jul 13). Purification and subunit interactions of yeast hexokinase. *Eur J Biochem, 28*(2), 241-252. https://doi.org/10.1111/j.1432-1033.1972.tb01907.x

Ferens, F. G., Patel, T. R., Oriss, G., Court, D. A., & Stetefeld, J. (2019, Mar 5). A cholesterol analog induces an oligomeric reorganization of VDAC. *Biophys J, 116*(5), 847-859. https://doi.org/10.1016/j.bpj.2019.01.031

Fernandez-Garcia, P., Pelaez, R., Herrero, P., & Moreno, F. (2012, Dec 7). Phosphorylation of yeast hexokinase 2 regulates its nucleocytoplasmic shuttling. *J Biol Chem, 287*(50), 42151-42164. https://doi.org/10.1074/jbc.M112.401679

Forte, M., Adelsberger-Mangan, D., & Colombini, M. (1987). Purification and characterization of the voltage-dependent anion channel from the outer mitochondrial membrane of yeast. *J Membr Biol, 99*(1), 65-72. https://doi.org/10.1007/BF01870622

Haloi, N., Wen, P. C., Cheng, Q., Yang, M., Natarajan, G., Camara, A. K. S., Kwok, W. M., & Tajkhorshid, E. (2021, Jun 3). Structural basis of complex formation between mitochondrial anion channel VDAC1 and Hexokinase-II. *Commun Biol, 4*(1), 667. https://doi.org/10.1038/s42003-021-02205-y

Hiller, S., Garces, R. G., Malia, T. J., Orekhov, V. Y., Colombini, M., & Wagner, G. (2008, Aug 29). Solution structure of the integral human membrane protein VDAC-1 in detergent micelles. *Science, 321*(5893), 1206-1210. https://doi.org/10.1126/science.1161302

Horney, M. J., Evangelista, C. A., & Rosenzweig, S. A. (2001, Jan 26). Synthesis and characterization of insulin-like growth factor (IGF)-1 photoprobes selective for the IGF-binding proteins (IGFBPS). photoaffinity labeling of the IGF-binding domain on IGFBP-2. *J Biol Chem, 276*(4), 2880-2889. https://doi.org/10.1074/jbc.M007526200

Kayikci, O., & Nielsen, J. (2015, Sep). Glucose repression in Saccharomyces cerevisiae. *FEMS Yeast Res, 15*(6). https://doi.org/10.1093/femsyr/fov068

Kelley, L. A., Mezulis, S., Yates, C. M., Wass, M. N., & Sternberg, M. J. (2015, Jun). The Phyre2 web portal for protein modeling, prediction and analysis. *Nat Protoc, 10*(6), 845-858. https://doi.org/10.1038/nprot.2015.053

Kovac, L., Nelson, B. D., & Ernster, L. (1986, Jan 14). A method for determining the intracellular distribution of enzymes in yeast provides no evidence for the association of hexokinase with mitochondria. *Biochem Biophys Res Commun, 134*(1), 285-291. https://doi.org/10.1016/0006-291x(86)90560-7

Kraakman, L. S., Winderickx, J., Thevelein, J. M., & De Winde, J. H. (1999, Oct 1). Structure-function analysis of yeast hexokinase: structural requirements for triggering cAMP signalling and catabolite repression. *Biochem J, 343 Pt 1*(Pt 1), 159-168. https://www.ncbi.nlm.nih.gov/pubmed/10493925

Kuser, P., Cupri, F., Bleicher, L., & Polikarpov, I. (2008, Aug). Crystal structure of yeast hexokinase PI in complex with glucose: A classical "induced fit" example revised. *Proteins, 72*(2), 731-740. https://doi.org/10.1002/prot.21956

Kuser, P. R., Krauchenco, S., Antunes, O. A., & Polikarpov, I. (2000, Jul 7). The high resolution crystal structure of yeast hexokinase PII with the correct primary sequence provides new insights into its mechanism of action. *J Biol Chem, 275*(27), 20814-20821. https://doi.org/10.1074/jbc.M910412199

Laurian, R., Dementhon, K., Doumeche, B., Soulard, A., Noel, T., Lemaire, M., & Cotton, P. (2019). Hexokinase and glucokinases are essential for fitness and virulence in the pathogenic yeast candida albicans. *Front Microbiol, 10*, 327. https://doi.org/10.3389/fmicb.2019.00327

Lazarus. N., Ramel, A., Rustum, Y., & Barnard, E. (1966, December 1, 1966). Yeast Hexokinase. I. Preparation of the Pure Enzyme. *Biochemistry, 5*(12), 4003-4016. https://doi.org/https://doi.org/10.1021/bi00876a035

Lemeshko, V. V. (2017, Nov). VDAC electronics: 4. Novel electrical mechanism and thermodynamic estimations of glucose repression of yeast respiration. *Biochim Biophys Acta Biomembr, 1859*(11), 2213-2223. https://doi.org/10.1016/j.bbamem.2017.09.001

Ma, H., Bloom, L. M., Dakin, S. E., Walsh, C. T., & Botstein, D. (1989). The 15 N-terminal amino acids of hexokinase II are not required for in vivo function: analysis of a truncated form

of hexokinase II in Saccharomyces cerevisiae. *Proteins, 5*(3), 218-223. https://doi.org/10.1002/prot.340050305

Magri, A., Reina, S., & De Pinto, V. (2018). VDAC1 as pharmacological target in cancer and neurodegeneration: focus on its role in apoptosis. *Front Chem, 6*, 108. https://doi.org/10.3389/fchem.2018.00108

Mazure, N. M. (2017, Aug). VDAC in cancer. *Biochim Biophys Acta Bioenerg, 1858*(8), 665-673. https://doi.org/10.1016/j.bbabio.2017.03.002

Meng, E. C., Goddard, T. D., Pettersen, E. F., Couch, G. S., Pearson, Z. J., Morris, J. H., & Ferrin, T. E. (2023, Nov). UCSF ChimeraX: Tools for structure building and analysis. *Protein Sci, 32*(11), e4792. https://doi.org/10.1002/pro.4792

Muller, D. J., Wu, N., & Palczewski, K. (2008, Mar). Vertebrate membrane proteins: structure, function, and insights from biophysical approaches. *Pharmacol Rev, 60*(1), 43-78. https://doi.org/10.1124/pr.107.07111

Neely, K. E., Hassan, A. H., Brown, C. E., Howe, L., & Workman, J. L. (2002, Mar). Transcription activator interactions with multiple SWI/SNF subunits. *Mol Cell Biol, 22*(6), 1615-1625. https://doi.org/10.1128/MCB.22.6.1615-1625.2002

Pastorino, J. G., & Hoek, J. B. (2008, Jun). Regulation of hexokinase binding to VDAC. *J Bioenerg Biomembr, 40*(3), 171-182. https://doi.org/10.1007/s10863-008-9148-8

Pastorino, J. G., Shulga, N., & Hoek, J. B. (2002, Mar 1). Mitochondrial binding of hexokinase II inhibits Bax-induced cytochrome c release and apoptosis. *J Biol Chem, 277*(9), 7610-7618. https://doi.org/10.1074/jbc.M109950200

Pelaez, R., Herrero, P., & Moreno, F. (2010, Nov 15). Functional domains of yeast hexokinase 2. *Biochem J, 432*(1), 181-190. https://doi.org/10.1042/BJ20100663

Piersimoni, L., Kastritis, P. L., Arlt, C., & Sinz, A. (2022, Apr 27). Cross-linking mass spectrometry for investigating protein conformations and protein-protein interactions horizontal line a method for all seasons. *Chem Rev, 122*(8), 7500-7531. https://doi.org/10.1021/acs.chemrev.1c00786

Randez-Gil, F., Sanz, P., Entian, K. D., & Prieto, J. A. (1998, May). Carbon source-dependent phosphorylation of hexokinase PII and its role in the glucose-signaling response in yeast. *Mol Cell Biol, 18*(5), 2940-2948. https://doi.org/10.1128/MCB.18.5.2940

Rao, V. S., Srinivas, K., Sujini, G. N., & Kumar, G. N. (2014). Protein-protein interaction detection: methods and analysis. *Int J Proteomics, 2014*, 147648. https://doi.org/10.1155/2014/147648

Roberts, D. J., & Miyamoto, S. (2015, Feb). Hexokinase II integrates energy metabolism and cellular protection: Akting on mitochondria and TORCing to autophagy. *Cell Death Differ, 22*(2), 248-257. https://doi.org/10.1038/cdd.2014.173

Rosano, C. (2011, May). Molecular model of hexokinase binding to the outer mitochondrial membrane porin (VDAC1): Implication for the design of new cancer therapies. *Mitochondrion, 11*(3), 513-519. https://doi.org/10.1016/j.mito.2011.01.012

Santangelo, G. M. (2006, Mar). Glucose signaling in Saccharomyces cerevisiae. *Microbiol Mol Biol Rev, 70*(1), 253-282. https://doi.org/10.1128/MMBR.70.1.253-282.2006

Scheuermann, T. H., Padrick, S. B., Gardner, K. H., & Brautigam, C. A. (2016, Mar 1). On the acquisition and analysis of microscale thermophoresis data. *Anal Biochem, 496*, 79-93. https://doi.org/10.1016/j.ab.2015.12.013

Schmidt, G. W., Welkenhuysen, N., Ye, T., Cvijovic, M., & Hohmann, S. (2020, Nov). Mig1 localization exhibits biphasic behavior which is controlled by both metabolic and regulatory roles of the sugar kinases. *Mol Genet Genomics, 295*(6), 1489-1500. https://doi.org/10.1007/s00438-020-01715-4

Schmidt, J. J., & Colowick, S. P. (1973, Oct). Chemistry and subunit structure of yeast hexokinase isoenzymes. *Arch Biochem Biophys, 158*(2), 458-470. https://doi.org/10.1016/0003-9861(73)90537-7

Schrödinger. (2023). *The PyMOL Molecular Graphics System.* In (Version 2.3.2) Schrödinger, LLC

Shoshan-Barmatz, V., Shteinfer-Kuzmine, A., & Verma, A. (2020, Oct 26). VDAC1 at the intersection of cell metabolism, apoptosis, and diseases. *Biomolecules, 10*(11). https://doi.org/10.3390/biom10111485

Summers, W. A., & Court, D. A. (2010, Jun). Origami in outer membrane mimetics: correlating the first detailed images of refolded VDAC with over 20 years of biochemical data. *Biochem Cell Biol, 88*(3), 425-438. https://doi.org/10.1139/o09-115

Uhlen, M., Fagerberg, L., Hallstrom, B. M., Lindskog, C., Oksvold, P., Mardinoglu, A., Sivertsson, A., Kampf, C., Sjostedt, E., Asplund, A., Olsson, I., Edlund, K., Lundberg, E., Navani, S., Szigyarto, C. A., Odeberg, J., Djureinovic, D., Takanen, J. O., Hober, S., Alm, T., Edqvist, P. H., Berling, H., Tegel, H., Mulder, J., Rockberg, J., Nilsson, P., Schwenk, J. M., Hamsten, M., von Feilitzen, K., Forsberg, M., Persson, L., Johansson, F., Zwahlen, M., von Heijne, G., Nielsen, J., & Ponten, F. (2015, Jan 23). Proteomics. Tissue-based map of the human proteome. *Science, 347*(6220), 1260419. https://doi.org/10.1126/science.1260419

Ujwal, R., Cascio, D., Colletier, J. P., Faham, S., Zhang, J., Toro, L., Ping, P., & Abramson, J. (2008, Nov 18). The crystal structure of mouse VDAC1 at 2.3 A resolution reveals mechanistic insights into metabolite gating. *Proc Natl Acad Sci U S A, 105*(46), 17742-17747. https://doi.org/10.1073/pnas.0809634105

Vega, M., Riera, A., Fernandez-Cid, A., Herrero, P., & Moreno, F. (2016, Apr 1). Hexokinase 2 Is an intracellular glucose sensor of yeast cells that maintains the structure and activity of Mig1 protein repressor complex. *J Biol Chem, 291*(14), 7267-7285. https://doi.org/10.1074/jbc.M115.711408

Yamashita, Y., Ashihara, H. (1988, June 28, 1988). Characterization of hexokinase and fructokinase from suspension-cultured catharanthus roseus cells. *Zeitschrift für Naturforschung 43c*, 827-834.